The University of Nottingham
School of Chemistry

Design and Development of Organic Electrocatalysts for CO_2 Reduction

Student Name: Fatin Altemani

Student ID Number:20518949

supervisors: Dr. Graham Newton and

Dr. Darren Walsh

Date: 30/09/2024

1. Abstract:

The electrochemical carbon dioxide reduction reaction (CO_2RR) represents a promising method for converting carbon waste streams into valuable chemicals. Current CO_2RR electrocatalysts often rely on expensive and rare platinum group metals, highlighting the need for more sustainable and cost-effective alternatives. This thesis explores the use of aromatic nitro group-bearing catalysts for the CO_2RR, focusing on their performance in different electrolyte systems. Cyclic voltammetry was employed to evaluate catalytic efficiency. Additionally, the influence of the electrolyte and gas environment (N_2 vs. CO_2) on the catalytic activity was investigated. Results demonstrated that aromatic nitro group catalysts exhibited improved CO_2 reduction activity in both electrolyte systems. This study provides insights into the relationship between catalyst structure, electrolyte composition, and gas environment, suggesting that further optimization of these catalyst-electrolyte systems could enhance the efficiency and selectivity of the CO_2RR, advancing sustainable chemical production processes.

Table of Contents

2. Introduction:

2.1. CO_2 emissions as a global issue:

The growing atmospheric carbon dioxide (CO_2) levels have recently become a significant environmental challenge.[1] Anthropogenic activities such as burning fossil fuels for energy generation, deforestation and agricultural practices release tonnes of extra CO_2 into the atmosphere. [2,3] CO_2 is the primary greenhouse gas responsible for global warming and is the major factor contributing to climate change. [4] The Industrial Revolution is widely acknowledged to have had a significant impact.[5] The widespread burning of fossil fuels such as coal and oil for energy production combined with the subsequent increase in industrialisation and transportation led to the deforestation of large areas and a significant rise in CO_2 emissions into the atmosphere.[6,7] Rising CO_2 levels are having an ongoing destabilising impact on Earth's climate.[8] Renewable energy sources such as solar, wind, hydroelectric, geothermal and bioenergy can effectively replace fossil fuels and significantly reduce CO_2 emissions.[9] Switching to a diverse range of other low emission technologies is essential for zero carbon energy options. This includes nuclear power and carbon capture and storage (CCS) systems which have the potential to provide power without directly emitting greenhouse gases.[10]

2.2. CO_2 reduction chemistry:

A pressing challenge is developing effective technologies for utilizing/converting CO_2 through thermal and electrochemical carbon dioxide reduction reactions, which require high energy levels and are inefficient.[11] Attempts are being made to transform CO_2 into usable fuel for chemical reactions to mitigate these and promote cleaner energy alternatives. Several methods have been demonstrated to convert CO_2 into useful products[12], including electrochemical[13], photochemical[14], radiochemical[15], and thermochemical approaches.[16] CO_2 is a relatively inert molecule and substantial energy input is required to drive its conversion to more valuable chemical products. This has led to extensive research into the development of efficient electrocatalysts for CO_2 reduction reactions (CO_2RR) under mild conditions. One of the difficulties in reducing CO_2 is its kinetic inertness. The one-electron reduction of CO_2 to $CO_2^{\bullet-}$ has an E^0 of -1.90 V vs. NHE (standard hydrogen electrode) at pH = 7 (equation (1). Besides CO_2's inherent chemical stability the electrochemical reduction of this greenhouse gas faces several other significant challenges that have motivated ongoing research. The competitive hydrogen evolution reaction (HER) can also coincide with CO_2 reduction impacting CO_2RR productivity and efficiency and HER (equation (7) is often preferred to CO_2 reduction in protic solvents.[17] While multiple proton-coupled electron transfers to CO_2 are thermodynamically less demanding (equations (2) to (6) they typically require large overpotentials even in the presence of catalysts. Additionally, CO_2 reduction may lead to CO, HCOOH, HCOH, CH_3OH, CH_4 or higher hydrocarbons.[18]

Moreover, practical applications require high selectivity but it can be challenging to achieve it. Similarly, it can be challenging to overcome the relatively low solubility of in polar solvents to ensure effective CO_2 delivery to the catalyst surface.[19] Overcoming these multifaceted challenges is essential to realizing electrochemical CO_2 reduction's full potential as a sustainable approach to converting this greenhouse gas into valuable chemicals and fuels.

Reaction	E^0 vs. NHE	Eq. No.
$CO_2 + e^- \rightarrow CO_2^{\bullet -}$	−1.90 V	(1)
$CO_2 + 2H^+ + 2e^- \rightarrow CO + H_2O$	−0.53 V	(2)
$CO_2 + 2H^+ + 2e^- \rightarrow HCO_2H$	−0.61 V	(3)
$CO_2 + 4H^+ + 4e^- \rightarrow HCHO + H_2O$	−0.48 V	(4)
$CO_2 + 6H^+ + 6e^- \rightarrow CH_3OH + H_2O$	−0.38 V	(5)
$CO_2 + 8H^+ + 8e^- \rightarrow CH_4 + 2H_2O$	−0.24 V	(6)
$2H^+ + 2e^- \rightarrow H_2$	0.00 V	(7)

Reduction Potentials of Carbon Dioxide Reactions

2.3. CO_2 reduction catalysis:

Electrocatalysis can reduce CO_2 using heterogeneous and homogeneous catalysts. The heterogeneous catalytic system typically consists of a transition metal alloy immobilized on a solid support that can be easily separated and recycled.[20] These catalysts often display high stability and can readily be integrated into electrochemical devices for continuous conversion. In addition to metal nanoparticles and metal-organic frameworks, transition metal oxides are promising catalysts for producing valuable chemicals and fuels from CO_2.[21,22] However, homogeneous catalysts such as molecular metal complexes or organic catalysts dissolved in an electrolyte can provide greater tunability and automatic insight into the reduction.[23] Because they are soluble these catalysts can be modified to tune their electronic and steric properties. However, to implement homogeneous systems the challenge of catalyst separation and recycling must be addressed.[24] To develop highly efficient and sustainable electrocatalytic CO_2 reduction technologies ongoing research efforts aim to combine the benefits of heterogeneous and homogeneous approaches. Figure 1 illustrates three pathways for electrochemical CO_2 reduction (CO_2R). In pathway A, CO_2 is directly reduced at the electrode to form CO_2 R products. Pathway B involves a catalyst (cat) that alternates between oxidised (cat_{ox}) and reduced (cat_{red}) states. The reduced catalyst with CO_2 to produce CO_2 products while the electrode regenerates the catalyst improving energy efficiency. Pathway C uses a mediator (Med) to shuttle electrons between the electrode and the catalyst enhancing the selectivity and efficiency of CO_2 reduction. Overall, the pathways show the progression from direct reduction to more efficient catalytic and mediator assisted processes.

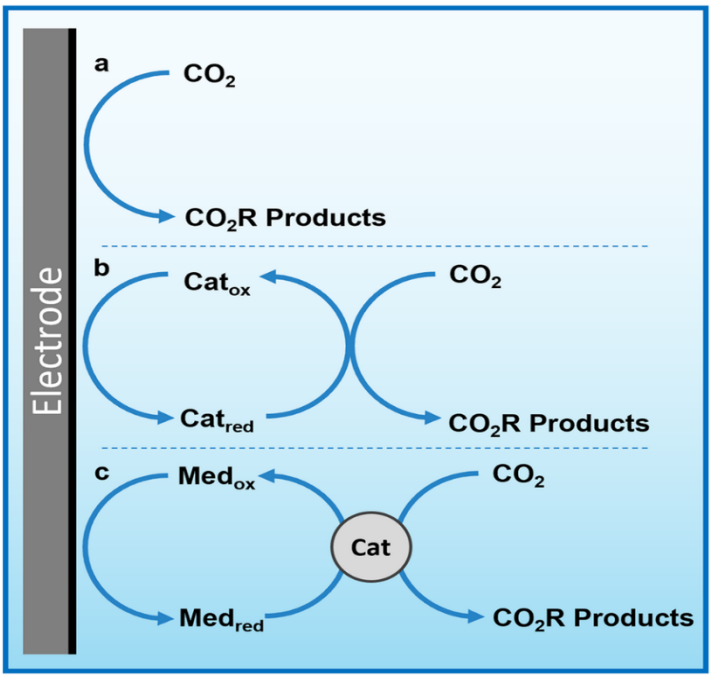

Figure 1. shows the Simplified mechanism of heterogeneous, homogeneous, and redox-mediated heterogeneous electrochemical CO_2 reduction. [25]

Examples of catalyst Electrocatalysts and photocatalysts can reduce CO_2 with high selectivity and efficiency minimize energy waste and increase sustainability.[26] As a result, electrocatalytic and photocatalytic CO_2 reduction processes can be conducted at room temperature and atmospheric pressure making them more energy-efficient and economically feasible than traditional methods which require high temperatures and pressures.[20] Due to their modularity and scalability electrocatalytic and photocatalytic systems can be used at various scales from small scale applications to extensive industrial facilities allowing them to be applied to multiple CO_2 emission sources.[27] Electrocatalytic and photocatalytic methods can create carbon neutral or carbon negative processes using renewable energy. They simultaneously remove carbon dioxide from the atmosphere while producing valuable chemicals and fuels.[28] Compared to photosynthesis electrocatalytic CO_2 reduction can achieve higher conversion efficiency with some systems achieving up to 80% efficiency when converting electrical energy into chemical energy stored in carbon reduction products.[27] Moreover, electrocatalytic methods allow greater control over the selectivity of CO_2 reduction products. Designing electrocatalytic reduction reaction cycles and enhancing the reaction conditions makes producing specific high value

chemicals such as carbon monoxide, formic acid, or ethylene possible.[13] Electrocatalytic CO_2 reduction can be carried out continuously as long as electricity and CO_2 are available. In contrast, photocatalytic reduction is restricted to daytime operation and depends on sunlight exposure.[29] Electrocatalytic methods can be used in industrial settings without requiring a large area of arable land which is especially important given the increasing global population and the limited availability of fertile land.[28] Electrocatalytic CO_2 reduction can achieve much faster reaction rates than photocatalytic reduction and convert CO_2 into valuable products using advanced electrocatalytic and optimized reactor designs.[20]

2.4. Examples of electrocatalysts:

A variety of catalyst systems each with unique characteristics can improve the electrochemical reduction of CO_2. For example, a range of transition metal coordination complexes comprising ligands such as pyridine, bipyridine, and porphyrins, can be used to selectively convert CO_2 to CO. Copper based complexes have demonstrated exceptionally high activity and selectivity for CO_2RR.[30] It has been shown that metal centers in coordination compounds can be effective electrocatalysts for various significant electrochemical reactions and are one of the most widely used electrocatalytic methods.[31]

In fuel cell technology oxygen reduction reaction (ORR) has been extensively studied using cobalt porphyrin complexes as electrocatalysts.[32] The research demonstrates that these complexes exhibit significant catalytic activity effectively facilitating the reduction of oxygen to water or hydrogen peroxide an essential reaction in the operation of fuel cells. Furthermore, the findings emphasize that cobalt being more abundant and less expensive than platinum offers a cost effective and sustainable alternative to the traditionally used platinum based catalysts. The stability and efficiency of cobalt porphyrin complexes position them as a promising candidate for future advancements in clean energy technologies particularly in developing more sustainable and economically viable fuel cells. Also, nickel ligands containing redox active ligands have proven to be effective electrocatalysts in the hydrogen evolution reaction (HER) which is one of the critical processes in producing hydrogen fuel.[33] These complexes efficiently convert protons to hydrogen gas benefiting from the enhanced electron transfer provided by the reversible redox reactions of the ligands. Nickel's abundance and lower cost compared to platinum make these complexes a cost effective and scalable option. Additionally, their stability under operating conditions ensures long term durability. These findings suggest that nickel complexes offer a promising sustainable alternative for efficient hydrogen production. Copper based ligands have been studied as electrocatalysts for the electrochemical reduction of carbon dioxide.[34] The research shows that these complexes efficiently convert CO_2 into hydrocarbons and alcohols, such as methane, ethylene, and ethanol, which are vital for industrial use. The catalytic activity is attributed to the stabilisation of intermediate species during the reduction process which improves efficiency and

selectivity. This approach not only aids in producing valuable chemicals but also contributes to CO_2 emission reduction aligning with climate change mitigation efforts.

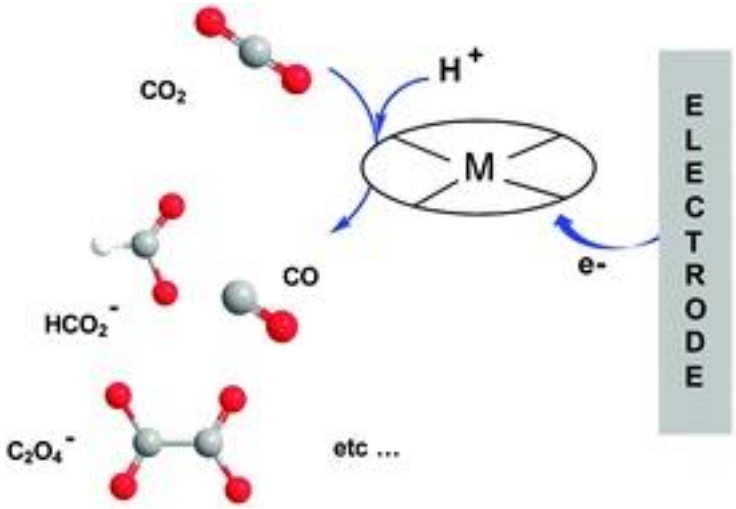

Figure 2. An electrochemical process in which CO_2 is electrochemically reduced at a redox active transition metal (M) complex to produce a range of products.[35]

2.5. Organic electrocatalysts:

On the other hand, organic electrocatalytic systems have emerged as a promising alternative to traditional inorganic catalysts for electrochemical applications. They have advantages over their inorganic counterparts including their efficiency, scalability, and environmental compatibility which makes them an attractive option for sustainable energy applications. Organic molecules are capable of catalysing significant redox reactions including water splitting, CO_2 reduction, and energy storage.[36] In response to the emergence of organic electrocatalysts researchers have begun to focus on these materials as organic molecules that can be designed and tailored at the molecular level. Compared to traditional inorganic complexes these selectively tuneable catalysts provide clear advantages in catalytic processes. Inorganic complexes cannot typically precisely control the outcome of a reaction often resulting in a mixture of products that require further separation and purification. On the other hand, tuneable catalysts can be designed to direct the response toward a specific product leading to higher yields of that desired product with fewer by products. This reduces the need for additional processing steps making the overall process more efficient and cost effective. Moreover, the versatility of tuneable catalysts allows them to be customized for a wide range of reactions offering greater adaptability for various industrial applications. This adaptability and enhanced efficiency make tuneable catalysts more sustainable and practical than conventional inorganic complexes. Molecular structure and properties can be tuned by adjusting the electronic structure adding functional groups and adding redox active centers among other strategies. They alter their catalytic properties including their redox behaviour and CO_2 activation to improve the efficiency and selectivity of product formation.[35] Understanding the fundamental design principles of organic electrocatalysts is key to developing effective organic electrocatalysts for CO_2 reduction. [37] The potential of organic molecules as effective catalysts for CO_2 reduction was detailed in a 2013 review in *Chemical Society Reviews*. The review identifies four key classes**:(1)** tetraalkylammonium These salts can act as co-catalysts or mediators enhancing the performance of primary catalysts in CO_2 reduction aromatic esters, **(2)** nitriles, **(3)** ionic liquids, and **(4)** pyridinium derivatives that can rival traditional metal-based catalysts in terms of selectivity and energy efficiency for CO_2 conversion. These findings suggest that organic molecules could be crucial in advancing sustainable CO_2 reduction technologies. [38]

2.6. Pyridine as electrocatalysts for CO_2 reduction:

In terms of the reduction of CO_2, organic electrocatalysts show great promise as new sustainable alternatives[39] Pyridinium compounds have proven to be effective and efficient in organic electrocatalyst synthesis. Organic molecules play an important role in CO_2 reduction by acting as hydrogen bond donors Brønsted acids and Lewis bases. As hydrogen bond donors they help stabilise reaction intermediates. As Brønsted acids (proton donors) and Lewis bases (electron pair donors) they enhance catalytic processes making CO_2 reduction more efficient. As hydrogen bond donors they can stabilise reaction intermediates leading to more efficient reaction pathways. When functioning as Brønsted acids they provide protons to the reaction which can increase the reactivity of CO_2 or related intermediates. As Lewis bases, they interact with CO_2 activating it and making it more prone to nucleophilic attack. This multifunctionality enables organic molecules to influence the reaction environment effectively improving selectivity and efficiency in CO_2 reduction. Such as the pyridine itself is redox active and therefore delivers the charge to the CO_2. Their ability to perform multiple roles makes them competitive with traditional metal based catalysts offering a more sustainable and adaptable approach to CO_2 conversion nitrogen containing heterocyclic compounds play a role in several catalytic processes.[40] It has also been utilized in pyridine dependent C-H activation reactions catalysed by platinum and palladium, allowing the selective functionalization of otherwise unreactive C-H bonds.[41] [42] Specifically, pyridinium salts have been extensively utilized for phase transfer to promote the reaction.

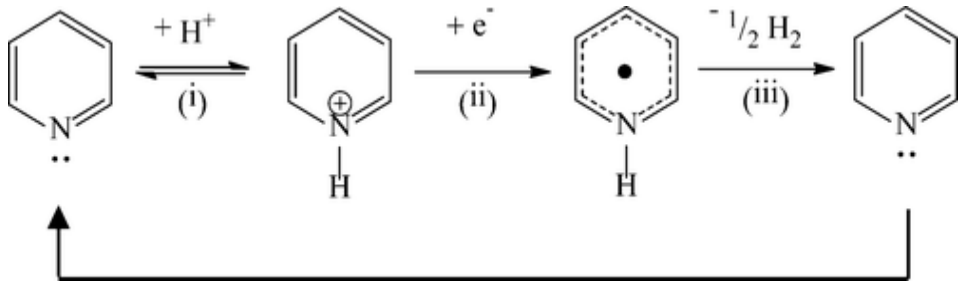

Figure 3. The pyridinium reduction mechanism, illustrating (i) protonation at lower pH, (ii) one-electron reduction to form the pyridinyl radical, and (iii) subsequent generation of dihydrogen and pyridine.[43]

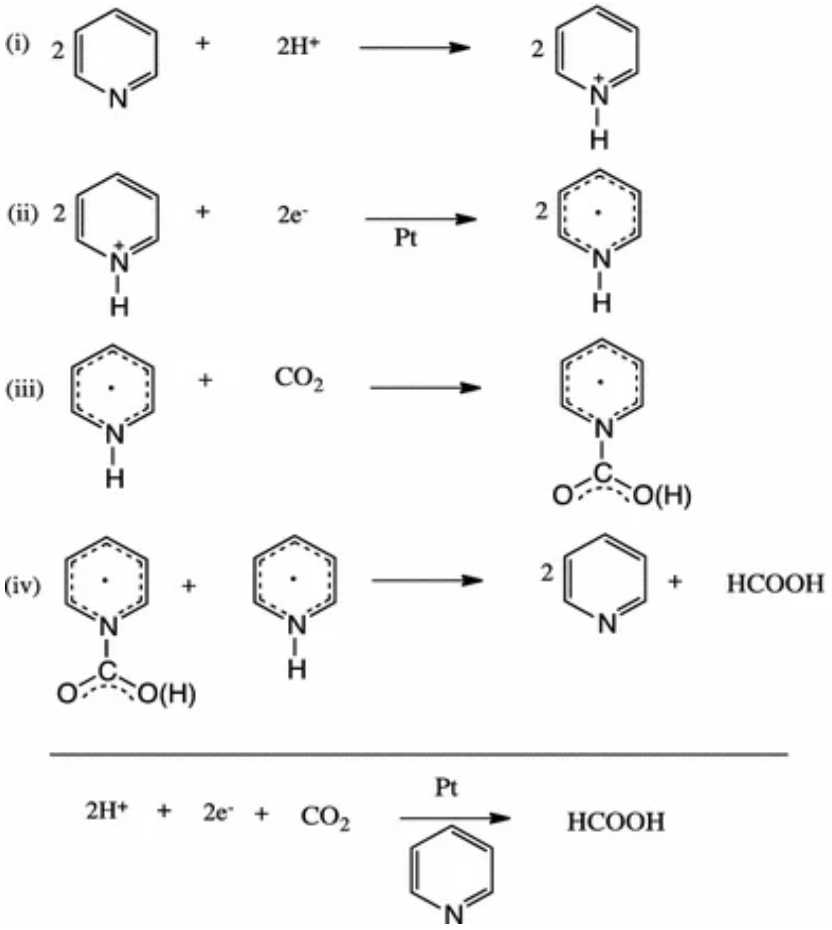

Figure 4. The proposed CO_2 reduction mechanism is based on the homogeneous reduction of PyrH+ to PyrH• (ii), followed by the formation of the carbamate intermediate (iii) and inner-sphere-type electron transfer from the pyridinium radical to the substrate (iv).[44]

2.7. Next directions for organic electrocatalysts:

Incorporating nitro-groups into pyridine-based catalysts has demonstrated promise in improving their performance in CO_2 reduction reactions by increasing the acidity of the pyridine ring. The electron-withdrawing nitro-group can facilitate the activation and reduction of CO_2.[45] Adding the nitro-group and other heterocyclic structures can promote the initial binding and adsorption of CO_2 on the catalyst surface since the ring is electron-deficient. As a result, the catalytic system can better capture and activate CO_2, a crucial step in the reduction process.[46] In CO_2 reduction reactions, pyridinium salts with nitro substituents provide improved catalytic activity and selectivity compared to their unsubstituted counterparts.[46] Even though the nitro substituted pyridine ring has an electron-deficient nature it is believed to promote the binding and activation of CO_2. The pyridine moiety may be a proton source for proton-coupled electron transfer.[47] The nitro group can also influence the orientation and stabilization of key reaction intermediates further improving catalytic efficiency.[48]By doing so, the CO_2 reduction reaction will become more selective and efficient promoting the formation of desired products such as carbon dioxide, hydrocarbons, or formate ions rather than competing hydrogen evolution.[49] Due to the complexity of synthesising pyridine derivatives with nitro groups this class of catalysts has been considered less attractive for converting CO_2 into valuable chemical feedstocks and fuels.

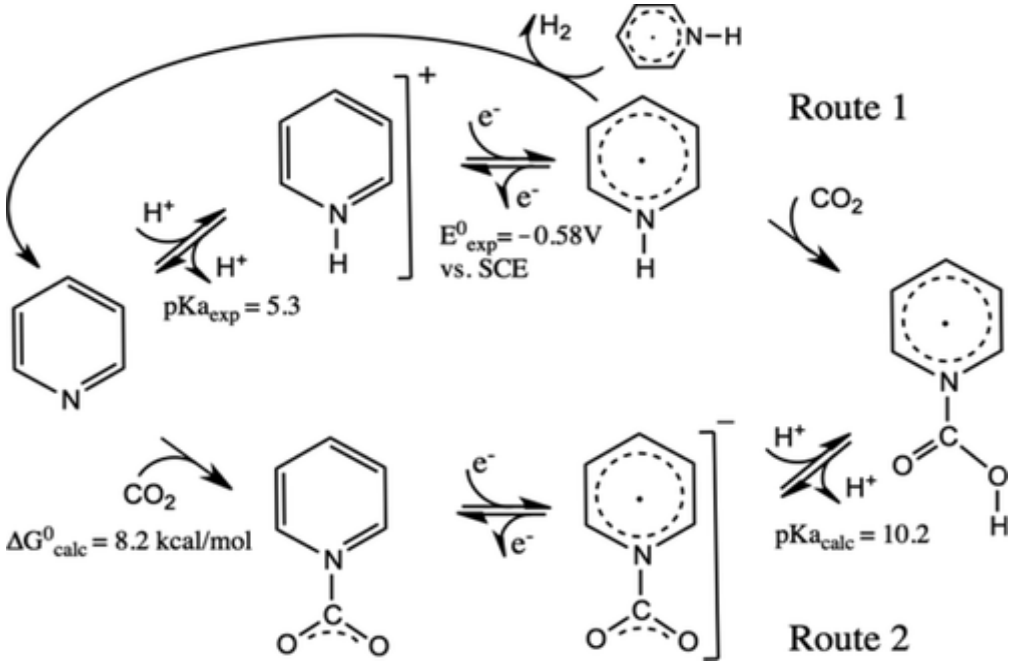

Figure 5. shows the Overall Proposed Mechanism for Pyridinium Reduction in CO_2 from Reactions.[50]

2.8. The Nitro group NO_2 role as catalysis for CO_2 reduction:

The use of certain functional groups can provide significant advantages in the electrochemical CO_2 reduction especially when considering the energy efficiency and economic viability.[51] As the CV analysis has revealed compounds that exhibit more reversible require lower overpotentials to drive the desired electrochemical reactions.[52,19] This is important advantage as each additional volt of potential needed represents a substantial increase in the operating costs of the CO_2 reduction.[53,27] That's mean minimizing the energy input is essential to keep energy consumption low and use affordable materials. As a result of that using the nitro group was necessary due to the NO_2 is a significant functional group in organic and inorganic chemistry due to its strong electron-withdrawing nature that affects selectivity and reactivity. By withdrawing electron density it acts as a powerful deactivator in electrophilic aromatic substitution and stabilises high-energy intermediates.[54] Additionally, the NO_2 group enhances acidity by stabilising conjugate bases which is crucial in catalyst design for metal organic frameworks and transition metal complexes. In the context of CO_2 reduction the ability of NO_2 to adjust redox potential is essential for activating CO_2 under less conditions when added to catalysts such as metal organic frameworks (MOFs) or metal complexes. Furthermore, NO_2 helps optimize the electronic environment around the catalyst making CO_2 reduction more efficient. [55] Because the position of the NO_2 significantly impacts electrochemical behaviour in the CV in the ortho position NO_2 the strong electron withdrawing leading to more negative reduction potentials and border CV peaks due to slower electron transfer. But in the meta position the effect is weaker causing moderate changes in the redox potential. In the para position NO_2 has the weaker resonance effect shifting the redox potential the most and leading to more apparent CV peaks. Overall, the position of the NO_2 influence both the redox potential and electron transfer.[51]

3. Three-electrode setup:

The three-electrode system is a widely used experimental arrangement in electrochemistry that offers a dependable and adaptable approach for investigating and regulating electrochemical processes. The system comprises three primary components.[24]

1- Working Electrode (WE):

The working electrode controls potential and measures current. The electrochemical reaction (oxidation/reduction) of interest occurs on the interface between the working electrode surface and the electrolyte/solution. Controlling and measuring the working electrode potential is done in relation to the reference electrode. Current flows between the counter electrode and the working electrode.[24]

2- Reference Electrode (RE):

An electrode with a stable and well-defined equilibrium potential. The working electrode potential is measured against the reference potential and the applied potential is reported against a specific reference. Standard hydrogen electrodes (SHE), silver/silver chloride electrodes (Ag/AgCl), and saturated calomel electrodes (SCE) are the most frequently used reference electrodes. The Nernst equation is typically used to determine the potential of the electrode[24]:

$$E = E^\circ - \frac{RT}{nF} \ln \frac{(Ox)}{(Red)} = E^\circ + 2.3026 \frac{RT}{nF} \log_{10} \frac{(Ox)}{(Red)}$$

Where (E) is the cell potential (electromotive force) at the temperature of interest, (E°) is the standard cell potential, (R) is the universal gas constant (8.314 $J \cdot K^{-1} \cdot mol^{-1}$), (T) is the temperature in kelvins, (n) is the number of moles of electrons transferred in the reaction, and (F) is the Faraday constant (approximately 96485 $C \cdot mol^{-1}$).

The Nernst equation establishes a connection between the potential (E) of an electrochemical cell and the standard potential (E^0) of a species as well as the relative activity of the oxidized (Ox) and reduced (Red) analyte in the system when it is in equilibrium. By considering the concentrations of the reactants and products this equation assists in determining the cell potential under various conditions.

3- Counter Electrode (CE):

The third electrode also referred to as the counter electrode completes the electrical circuit by facilitating the passage of current/flow of charge. The counter electrode is typically composed of an inert material such as platinum or graphite and is intended to have a significantly larger surface area than the working electrode. This is done to prevent the electrochemical reaction at the counter electrode from impacting the overall process[24]. Its primary function is to complete the circuit by allowing the equal and opposite current to working and prevent current from passing through the reference electrode which would alter the stable potential it would no longer be a reference. This is why we need a 3-electrode setup.

The three-electrode approach enables accurate adjustment and assessment of the working electrode potential regardless of how much the current runs through the cell. This setup is crucial for various electrochemical methods including potentiometry voltammetry, and electrochemical resistance spectroscopy. These techniques are widely used in fields such as energy storage, corrosion research, and electroanalytical chemistry.

This study has applied Cyclic Voltage Metering (CV) to investigate the electrochemical properties and behaviours of various organic electrocatalysts.

An overview of the fundamental principles of Cyclic Voltammetry shows that the potential of a working electrode is cycled linearly with time between two set values. By measuring the current a voltammogram can be generated revealing the analyte's electrochemical properties.[24]

Electrochemical Instrumentation:

For the cyclic voltammetry (CV) experiments in this study a CH700D potentiostat was used. This instrument allowed precise control over the voltage applied to the electrochemical cell and accurate current measurement. Also, a computer with instrument control software. The data collected from the CV scans was analysed using the Origin software program. This software made it easy to create high-quality graphs of the cyclic voltammograms.

Studies were carried out on nuclear magnetic resonance (NMR a400 MHz).

4.The Aim of This Project:

The purpose of this project will be to design and develop simple organic electrocatalysts for CO_2 reduction and evaluate their performance.

The inclusion of nitro moieties in pyridine derivatives has been shown to tune the catalytic performance of the system. However, relatively little is known about the potential for redox active nitro groups to work as CO_2RR electrocatalysts in their own right.

This project aims to investigate (i) the redox properties of aliphatic and aromatic nitro-bearing molecules; (ii) to explore the use of organic nitro groups as electrocatalysts for the CO_2RR.

Aromatic:

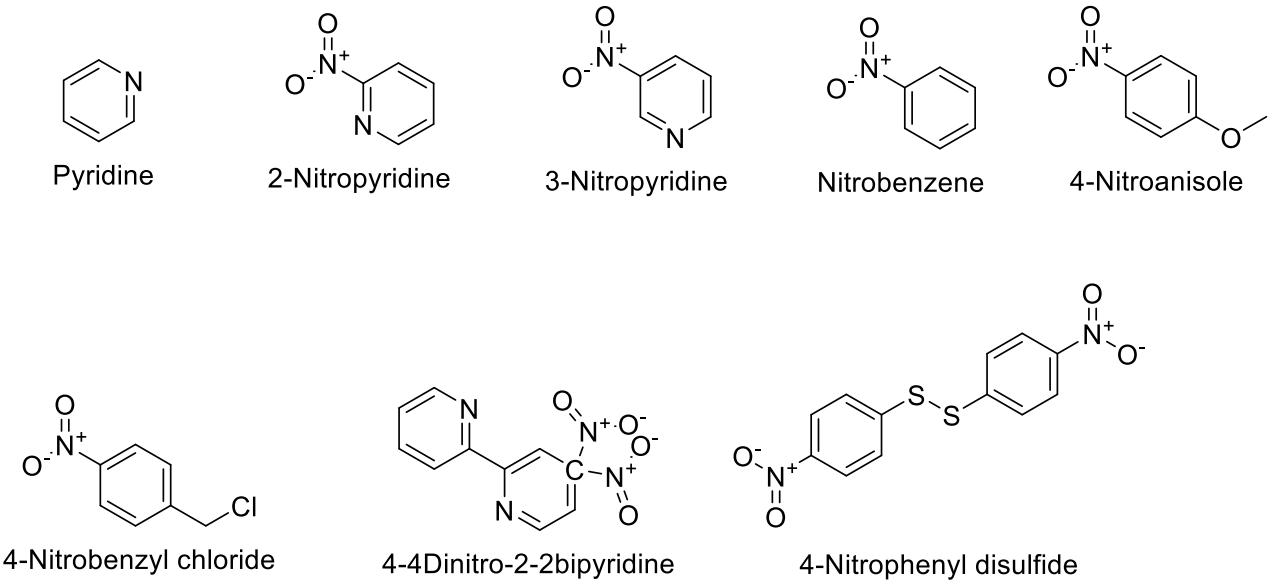

Figure 6. a structure of the organic molecular Aromatic.

Aliphatic:

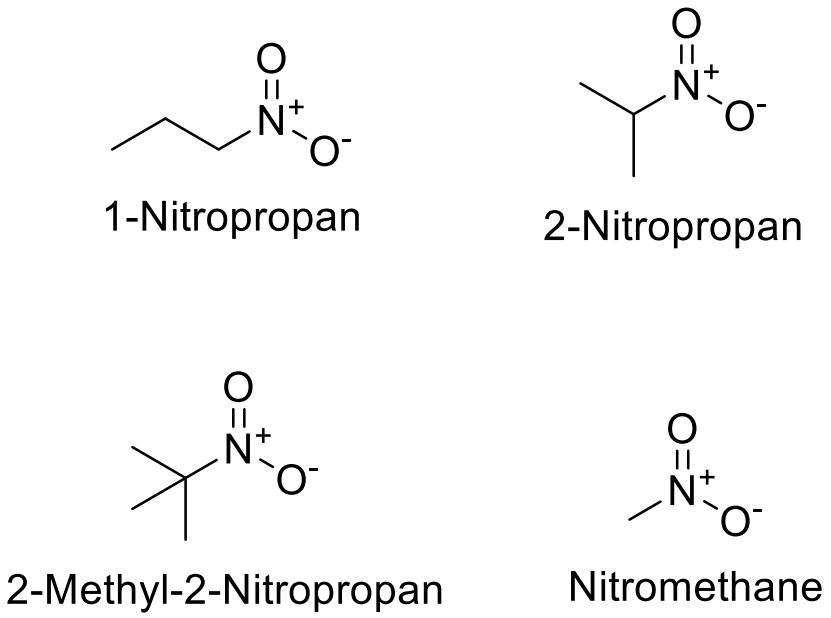

Figure 7. a structure of the organic molecular Aliphatic.

5. Experimental Methods

All chemicals were obtained from Sigma-Aldrich or Thermo Scientific in this experiment.

5.1. Cell configuration:

Working electrode:

The procedures were performed under a fume hood while wearing suitable personal protective equipment. The cell was prepared with a three-electrode setup comprising a glassy carbon (GC) working electrode, a silver (Ag) wire reference electrode, and a platinum (Pt) counter electrode. The working electrode was polished with three different grades of alumina (1 µm, 0.5 µm, and 0.03 µm) and rinsed with milli-Q water.

Reference electrode:

In the first two experiments, Ag wire used as the reference electrode was lightly polished on the surface using sandpaper.

Silver/silver nitrate reference electrode for the non-aqueous cell:

The Ag/$AgNO_3$ reference electrode was prepared by adding $AgNO_3$ (16.99 mg) to acetonitrile (MeCN) 10mL. A silver wire was inserted into a glass casing and heat shrink tubing sealed in the frit was inserted into the end and carefully heated. The electrode body was carefully filled with the prepared $AgNO_3$/MeCN solution taking care to avoid forming air bubbles.[24]

Saturated Calomel reference Electrode for the aqueous cell:

For electrochemical measurements in aqueous $KHCO_3$ solution, a Saturated Calomel Electrode (SCE) was used as the reference electrode. The SCE was chosen for its stable potential in aqueous media, with a standard potential of +0.241 V vs. the Standard Hydrogen Electrode (SHE) at 25 °C. The SCE was inserted directly into the electrochemical cell containing the $KHCO_3$ solution.[24]

Figure 8. Electrochemical cells with three electrodes set up.

5.2. The electrochemical cell preparation:

Cyclic Voltammetry (CV) was carried out in both aqueous (0.1 M $KHCO_3$ in water) and non-aqueous (0.1 M $TBAPF_6$ in acetonitrile) conditions using a CHI700D potentiostat. A working electrode (GC), the counter electrode (Pt), and the reference electrode (SCE for aqueous or Ag, $AgNO_3$ for non-aqueous systems) were used for all measurements. All electrode tips were adequately immersed in the electrolyte solution without touching each other.

The system was initially purged with nitrogen (N_2) gas to remove dissolved oxygen and create an inert atmosphere. The same setup was used to perform measurements under a CO_2 atmosphere and the electrolyte solution was thoroughly purged with CO_2 gas to ensure saturation. CV experiments were conducted under an inert atmosphere/condition for each catalyst in the aqueous ($KHCO_3$) and non-aqueous ($TBAPF_6$ in MeCN) electrolyte systems. All the graphs presented in this study were generated using OriginLab.

5.3. Electrolyte Preparation:

Non – aqueous electrolyte MeCN $TBAPF_6$ 0.1M:

A 0.1M solution of $TBAPF_6$ in MeCN (100 mL) was prepared by dissolving $TBAPF_6$ (3.87 g) in acetonitrile (100 mL) at room temperature.

Aqueous electrolyte potassium bicarbonate ($KHCO_3$) 0.1M:

Potassium bicarbonate ($KHCO_3$) (1.00 g) was dissolved in 1000L of distilled water and mixed until the solid had fully dissolved.

5.4. Ferrocene (C_{10} H_{10} Fe):

Ferrocene was used in all the molecular systems to compare the reversibility of the nitro-containing organic compounds to a stable reference.

Furthermore, all systems provide a point of comparison for evaluating the reversibility of the redox processes in the nitro-containing organic compounds. Incorporating ferrocene as a reference provides valuable insights into their potential applications, such as electrochemical CO_2 reduction catalysis.

5.5. Tetrabutylammonium hexafluorophosphate recrystallisation:

Tetrabutylammonium hexafluorophosphate ($TBAPF_6$) was recrystallised to produce high-purity material for the electrochemical analysis. $TBAPF_6$ (10 g) was weighed and transferred to an Erlenmeyer flask. The flask was additionally placed on a heater that included a stirrer. Ethanol 150mL was slowly added to $TBAPF_6$ 10g and heated 80°until the solid had fully dissolved and left overnight to crystallise. This was filtered via Buchner filtration into cold ethanol (150 mL). The filtered solid was washed three times with cold ethanol 150ml and left to dry for one hour under a vacuum. The purified sample of 9.74g was collected.

Figure 9. Purification of TBAPF6.

5.6. The organic catalysts that have been used in this experiment:

All the procedures were carried out under a fume hood while wearing suitable personal protective equipment.

5.6.1. Aliphatic catalysts:

1- 1-Nitropropan ($C_3H_7NO_2$)

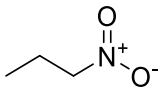

The electrolyte was prepared by dissolving 1-Nitropropane (898 µL) in 0.1 M $TBAPF_6$ in MeCN (10 mL).

2- 2-Nitropropan ($C_3H_7NO_2$)

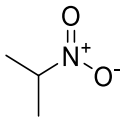

The electrolyte was prepared by dissolving 2-Nitropropane (907 µL) in 0.1 M $TBAPF_6$ in MeCN (10 mL).

3- Nitromethane (CH_3NO_2)

The electrolyte was prepared by dissolving Nitromethane (536 µL) in 0.1 M $TBAPF_6$ in MeCN (10 mL).

4- 2-Methyl-2-nitropropan ($C_4H_9NO_2$)

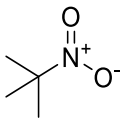

The electrolyte was prepared by dissolving 2-Methyl-2-nitropropane (103.12 mg) in 0.1 M $TBAPF_6$ in MeCN (10 mL).

5.6.2. Aromatic catalysts:

The procedures were carried out under a fume hood while wearing suitable personal protective equipment. To evaluate their performance under different conditions, all aromatic catalysts used in this study were prepared in both aqueous and non-aqueous systems. The aqueous medium consisted of 0.1 M $KHCO_3$ in water. The same catalysts were dissolved in a 0.1 M $TBAPF_6$in MeCN in the non-aqueous medium. The concentration of each catalyst remained consistent across both electrolyte systems to ensure that results were comparable. This approach allowed insights into the catalyst's redox behaviour in both aqueous and organic environments.

1- 2-Nitropyridine ($C_5H_4NO_2$)

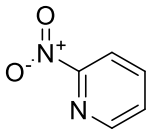

The electrolyte was prepared by dissolving 2-nitropyridine (124.1 mg) in 0.1 M $TBAPF_6$ in MeCN (10 mL).

2- 3-Nitropyridine ($C_5H_4N_2O_2$)

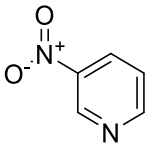

The electrolyte was prepared by dissolving 3-Nitropyridine (124.1 mg) in 0.1 M $TBAPF_6$ in MeCN (10 mL).

3- Pyridine (C_5H_5N)

The electrolyte was prepared by mixing pyridine (805 μL) with 0.1 M $TBAPF_6$ in MeCN (10 mL).

4- Nitrobenzene ($C_6H_5NO_2$)

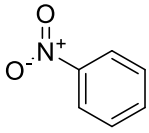

The electrolyte was prepared by mixing Nitrobenzene (1027 µL) with 0.1 M $TBAPF_6$ in MeCN (10 mL).

5- 4-Nitroanisole ($C_7H_7NO_3$)

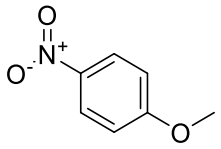

The electrolyte was prepared by dissolving 4-nitroanisole (153.14 mg) in 0.1 M $TBAPF_6$ in MeCN (10 mL).

6- 4-Nitrobenzyle chloride ($C_7H_6ClNO_2$)

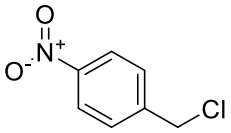

The electrolyte was prepared by dissolving 4-nitrobenzyl chloride (171.57 mg) in 0.1 M $TBAPF_6$ in MeCN (10 mL).

7- 4-4Dinitro-2-2bipyridine ($C_{10}H_6N_4O_4$)

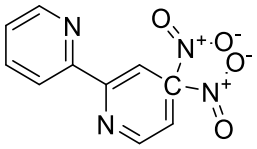

The electrolyte was prepared by dissolving 4,4'-dinitro-2,2'-bipyridine (272.22 mg) in 0.1 M $TBAPF_6$ in MeCN (10 mL).

8- 4-Nitrophenyl disulfide ($C_{12}H_8N_2O_4S_2$)

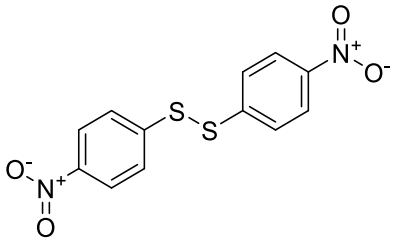

The electrolyte was prepared by dissolving 4-Nitrophenyl disulfide (308.34 mg) was accurately weighed and transferred to the volumetric flask, which was then filled with the MeCN $TBAPF_6$ to 10 mL.

5.7. Cyclic Voltammetry in a H-Cell:

The H-cell setup consisted of two compartments separated by a Celgard membrane compatible with MeCN. The Celgard membrane is composed of polypropylene (PP) a cost-effective and highly inert polymer. It withstands extreme pH environments and remains insoluble in most solvents at room temperature.[56] One compartment contained a solution of 0.1 M $TBAPF_6$ in MeCN 20 mL with 2-nitropyridine as the catalyst, a carbon mesh working electrode, and an $AgNO_3$ reference electrode. This compartment was saturated with CO_2 gas. The other compartment contained a solution of 0.1 M $TBAPF_6$ in MeCN 20 mL with no catalyst and a carbon mesh counter electrode.

Cyclic Voltammetry (CV) experiments were conducted at a scan rate of 200 mV/s for 100 cycles. These measurements were performed across a range of potential windows to explore the electrochemical behaviour of the system at lower/higher potentials/wider windows. After completion of the CV cycles, samples were carefully extracted from the electrolyte solution in the working electrode compartment. The amount of 0.5 mL for these samples was then prepared for NMR analysis. This technique allowed for a comprehensive study of the catalytic activity and product formation from the electrochemical reduction of CO_2 in the presence of a 2-nitropyridine catalyst.

5.8. ^{1}H NMR measurements:

Nuclear Magnetic Resonance (NMR a400 MHz) measurement was conducted to determine the contents of the electrolyte solution during the electrochemical reaction under CO_2 saturation. ^{1}H NMR, ^{31}P, and ^{18}F spectra provided detailed information about the molecular structures of the reaction products.

After the cyclic voltammetry experiments, an aliquot of electrolyte was extracted from the working electrode compartment of the H-cell. Deuterated dimethyl sulfoxide (DMSO-d_6) (0.1 mL) was added to the electrolyte solution (approx. 0.5 mL) and gently mixed.

This procedure was repeated using 4-nitroanisole, 3-nitropyridine, and nitrobenzene as catalysts, as these were considered the most interesting molecules for the experiments. All the graphs presented in this study were generated using Mnova.

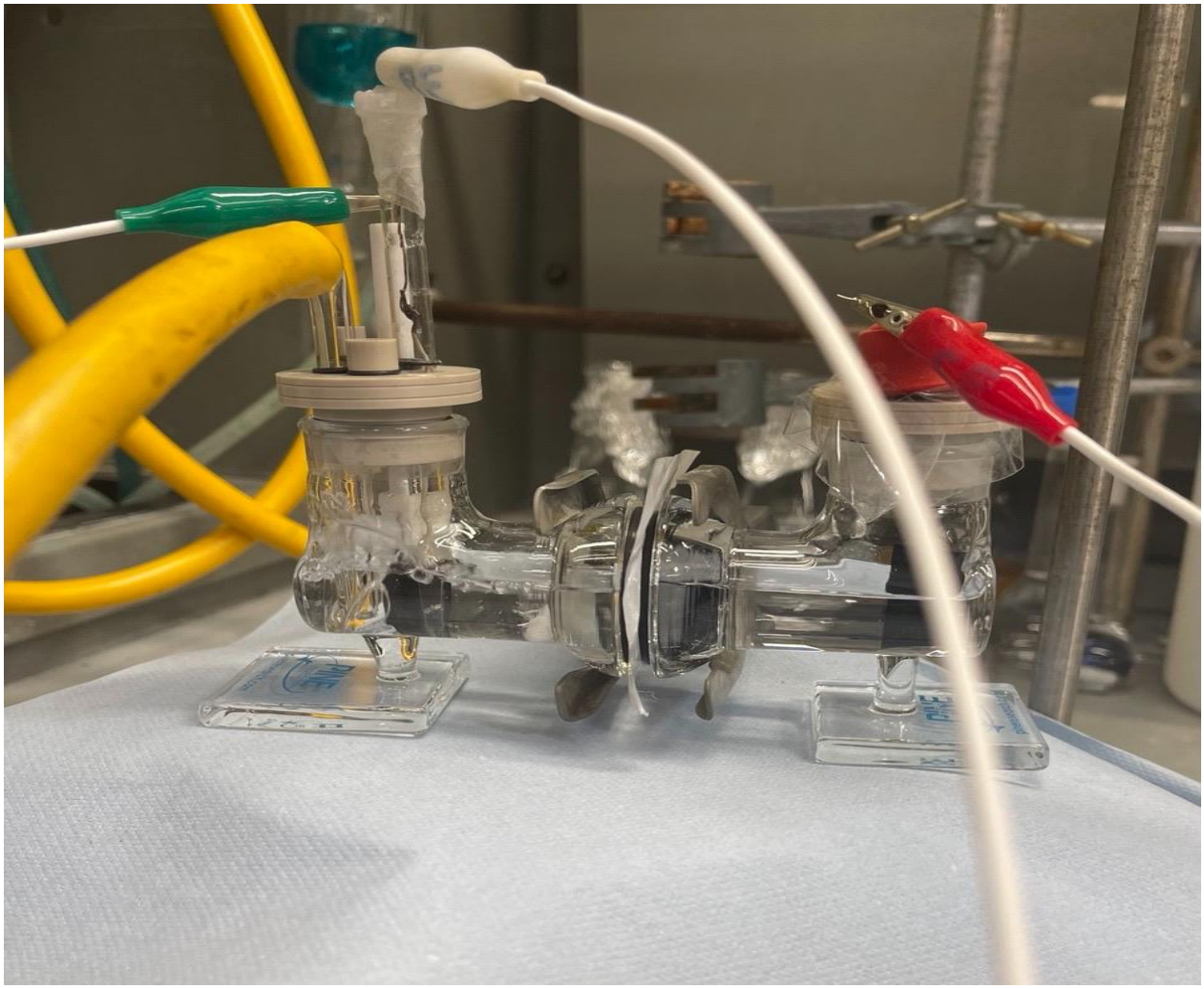

Figure 10. the H-cell experimental set-up.

6. Results and discussion:

6.1. Cyclic voltammetry (CV):

Cyclic voltammeter is a widely employed electro analytical technique well-suited for investigating the redox behaviour of organic compounds particularly those containing redox-active functional groups such as nitro-moieties.[51] This method is used to study the reduction and oxidation processes occurring at the electrode surface providing valuable information about the thermodynamics and kinetics of the underlying electrochemical reactions. Conducting cyclic voltammetry experiments provides insight into how experimental conditions such as the presence of specific reagents or gases can influence the redox transformations of the target compounds.[57] The electrochemical behaviour of the molecules under inert (N_2) and CO_2-rich environments indicates whether or not they may be involved in electrocatalysis of the CO_2RR.

6.1.1 Nonaqueous electrolytes with aliphatic catalysts under N_2:

Voltametric measurements were first carried out on aliphatic catalysts in a non-aqueous solution under N_2 to fully understand their electrochemical properties. This helped determine important details such as, their redox behaviour and catalytic activity. Each compound demonstrates unique redox characteristics because of their unique molecular structure and the various substituents attached to the nitro group.

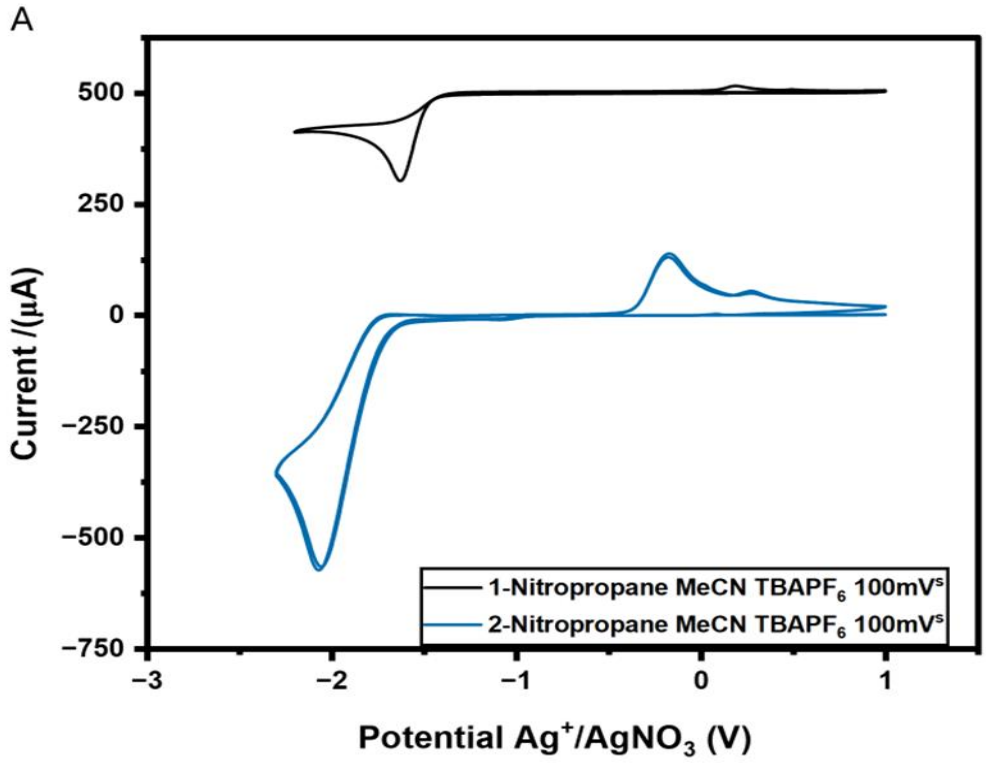

Figure11.(A) 1-nitropropane and 2-nitropropane as catalytic in MeCN $TBAF_6$ under N_2.

Figure 11. (A) shows 1-nitropropane (black curve) and 2-nitropropane (blue curve) with different redox behaviours. 2-nitropropane has clear reduction and oxidation peaks but the gap between them suggests that some structural changes occur during the redox process not fast electron transfer. On the other hand, 1-nitropropane shows very little current indicating weak or no redox activity likely meaning the process is irreversible.

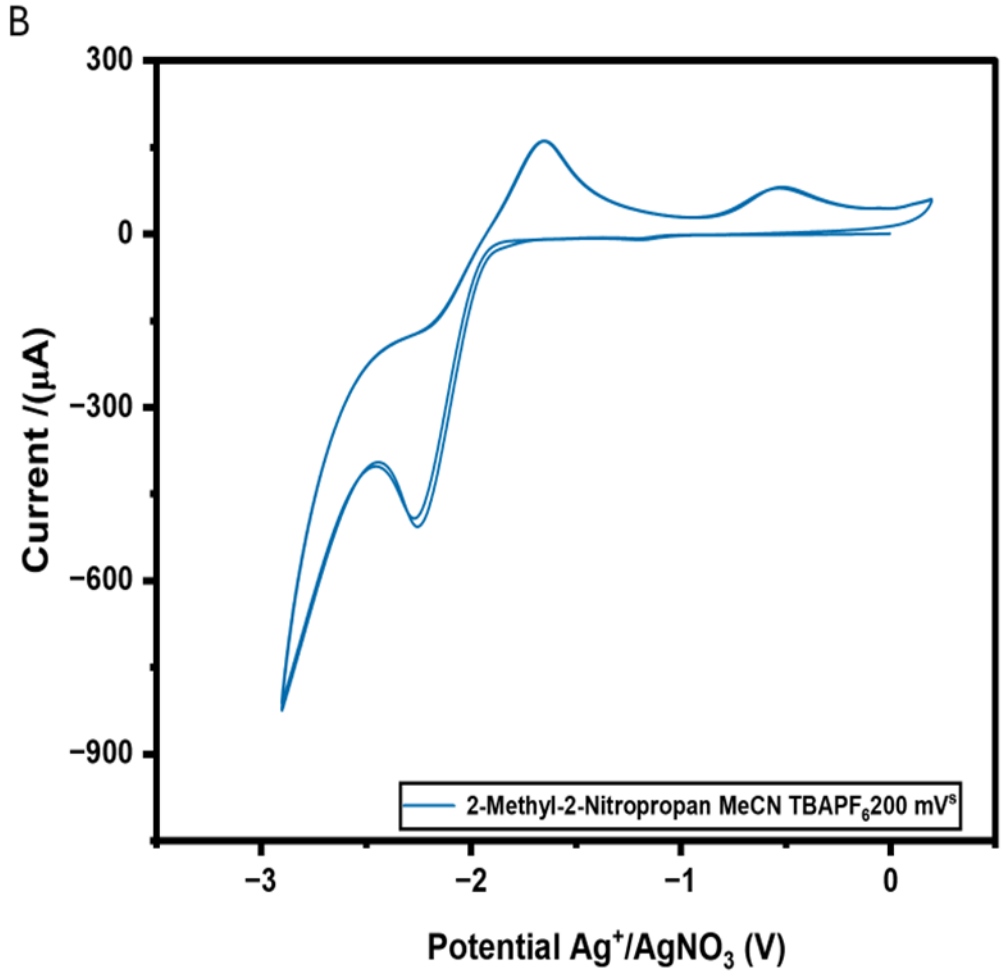

Figure12. (B) 2-methyl-2-nitropropane as catalytic in MeCN $TBAPF_6$ under N_2.

While in figure 12. (B) The curve displays apparent reduction and oxidation peaks indicating significant electron transfer activity. However, the separation between the reduction (around -2.5 V) and oxidation peaks suggests some structural changes during the redox process rather than fast electron transfer. The defined peaks suggest a quasi-reversible process where the electron transfer is noticeable but not completely reversible. This behaviour indicates that while 2-methyl-2-nitropropane undergoes significant electron transfer the process is not fully reversible.

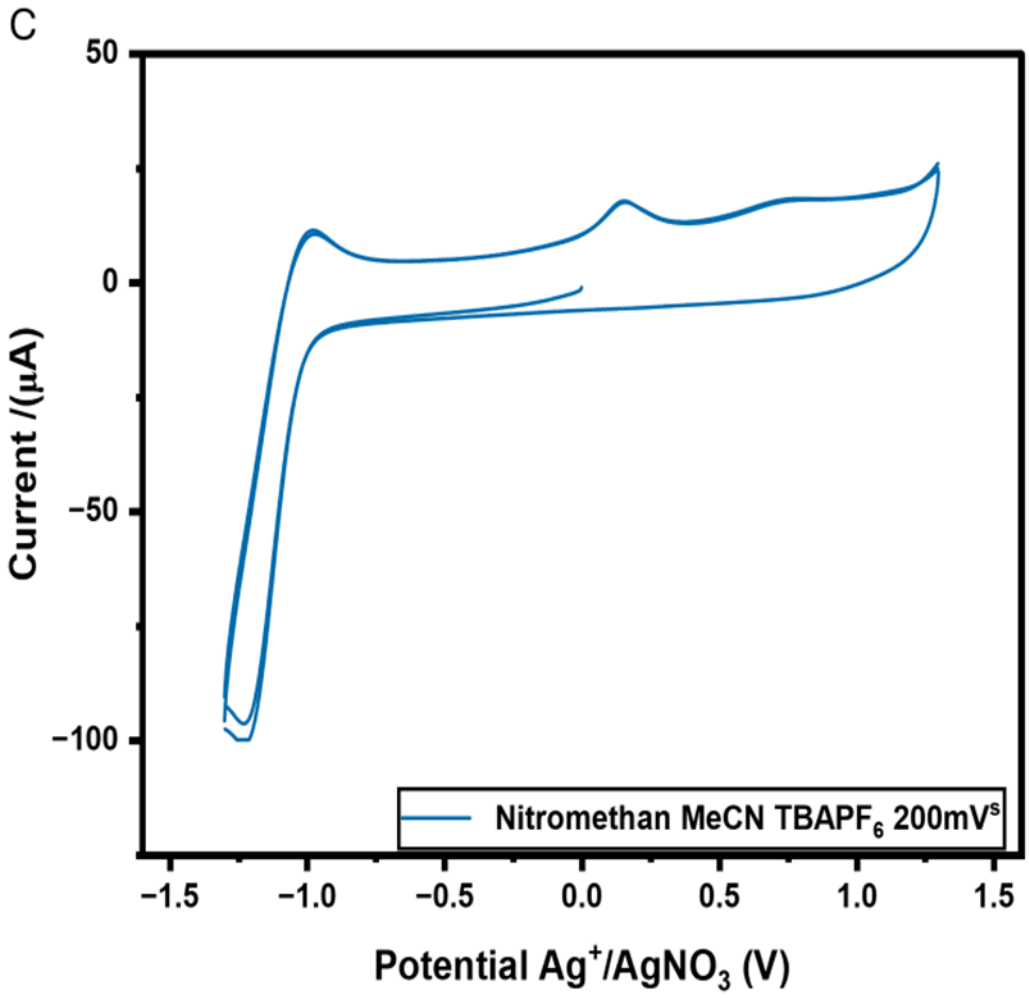

Figure13. (C) nitromethane as catalytic in MeCN $TBAPF_6$ under N_2.

Figure 13. (C**)** indicates much smaller and less pronounced redox peaks indicating a more reversible electron transfer process and less structural change during the redox cycle.

In comparing the redox behaviour for the aliphatic group 2-nitropropane and 2-methyl-2-nitropropane show clear reduction and oxidation peaks with significant peak separation, indicating strong electron transfer but quasi-reversible behaviour. The large peak separation suggests structural changes occur during the electron transfer preventing full reversibility. In contrast, 1-nitropropane displays minimal redox activity implying limited electron transfer. Because the lack of an aromatic ring in 1-nitropropan and 2-nitropropan contributes to their irreversibility. Without the electron delocalization and stabilization provided by an aromatic ring these aliphatic compounds undergo more drastic structural changes during redox reactions which reduces their ability to return to their original state after electron transfer.
Nitromethane exhibits small redox peaks with minimal peak separation indicating a more reversible electron transfer process though the smaller current values suggest weaker electron transfer compared to the other compounds.
Overall, 2-nitropropane and 2-methyl-2-nitropropane demonstrate substantial electron transfer with quasi-reversible behaviour while nitromethane shows more reversible electron transfer. 1-nitropropane exhibits very weak or no redox activity suggesting limited involvement in the electron transfer process. In addition, The -NO_2 group in aliphatic compounds remains strongly electron-withdrawing but without an aromatic system to stabilize the resulting intermediates the molecule cannot easily return to its original state. This limits the reversibility of the redox process.

6.1.2 Nonaqueous electrolytes with aromatic catalysts under N_2:

Voltametric measurements were carried out on aromatic catalysts in a non-aqueous solution under N_2 to fully understand their electrochemical properties. This helped determine important details such as, their redox behaviour and catalytic activity. Each compound demonstrates unique redox characteristics because of their unique molecular structure and the various substituents attached to the nitro group.

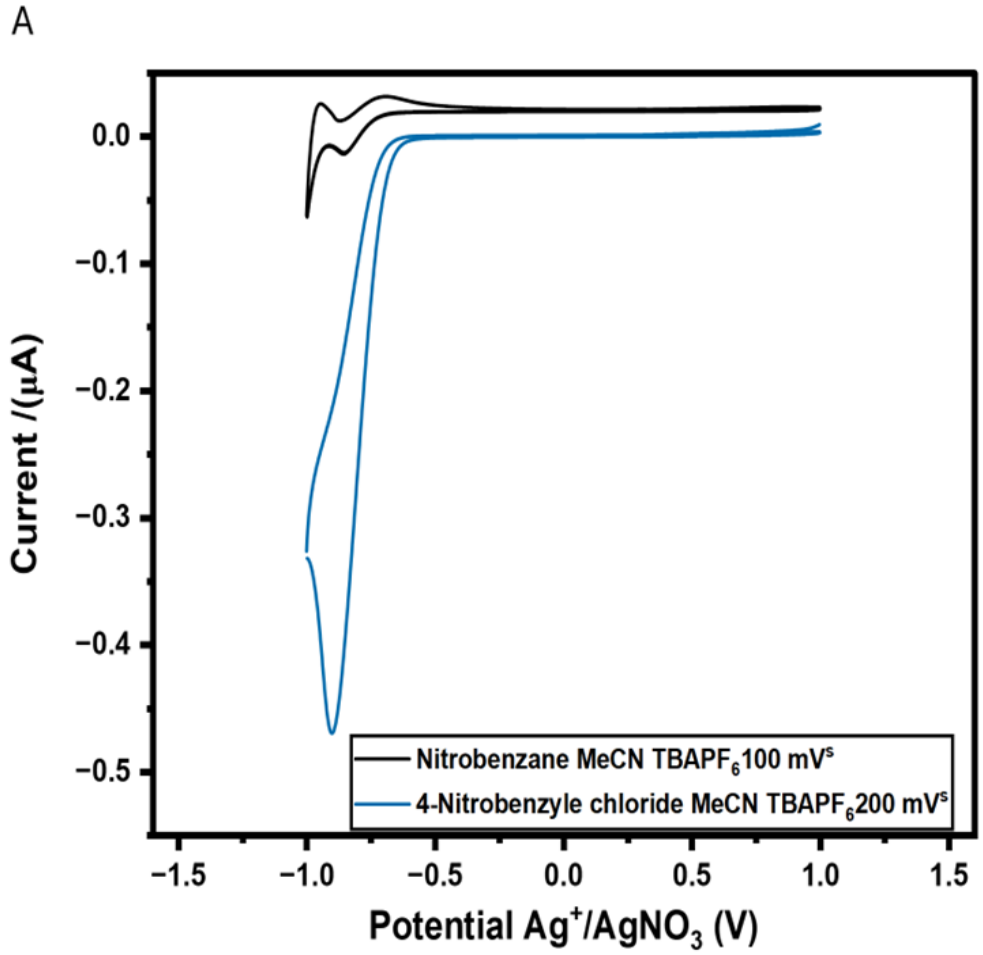

Figure14. (A) nitrobenzene and 4-nitrobenzyle chloride as catalytic in MeCN $TBAPF_6$ under N_2.

Figure 14. (A) show that nitrobenzene is characterized by its strong electron-withdrawing nitro group which dominates its reactivity and electrochemical behavior. The nitro group makes nitrobenzene more electrophilic and capable of undergoing reversible reduction in electrochemical processes. The conjugated aromatic system of the benzene ring helps stabilise the intermediates formed during redox reactions contributing to the compound's relative stability and reversibility in. In contrast, 4-nitrobenzyl chloride exhibits a more pronounced reduction peak around -1 V and significantly larger current indicating stronger electrochemical activity and more substantial electron transfer. The presence of the benzyl chloride group likely enhances the redox behaviour making the compound more electroactive compared to nitrobenzene**.** This may be because an electron-withdrawing effect which makes the benzyl group (-CH_2Cl) more electrophilic and reactive in nucleophilic substitution reactions. However, in terms of electrochemical behaviour the nitro group primarily governs the redox properties and the chlorine atom has a relatively minor indirect influence. The presence of chlorine contributes to the molecule's overall reactivity but does not drastically affect the reversibility of the redox process dominated by the nitro group. Both compounds follow relatively reversible processes as indicated by the minimal separation between reduction and oxidation peaks but 4-nitrobenzyl chloride shows a much stronger redox response highlighting its greater involvement in electron transfer.

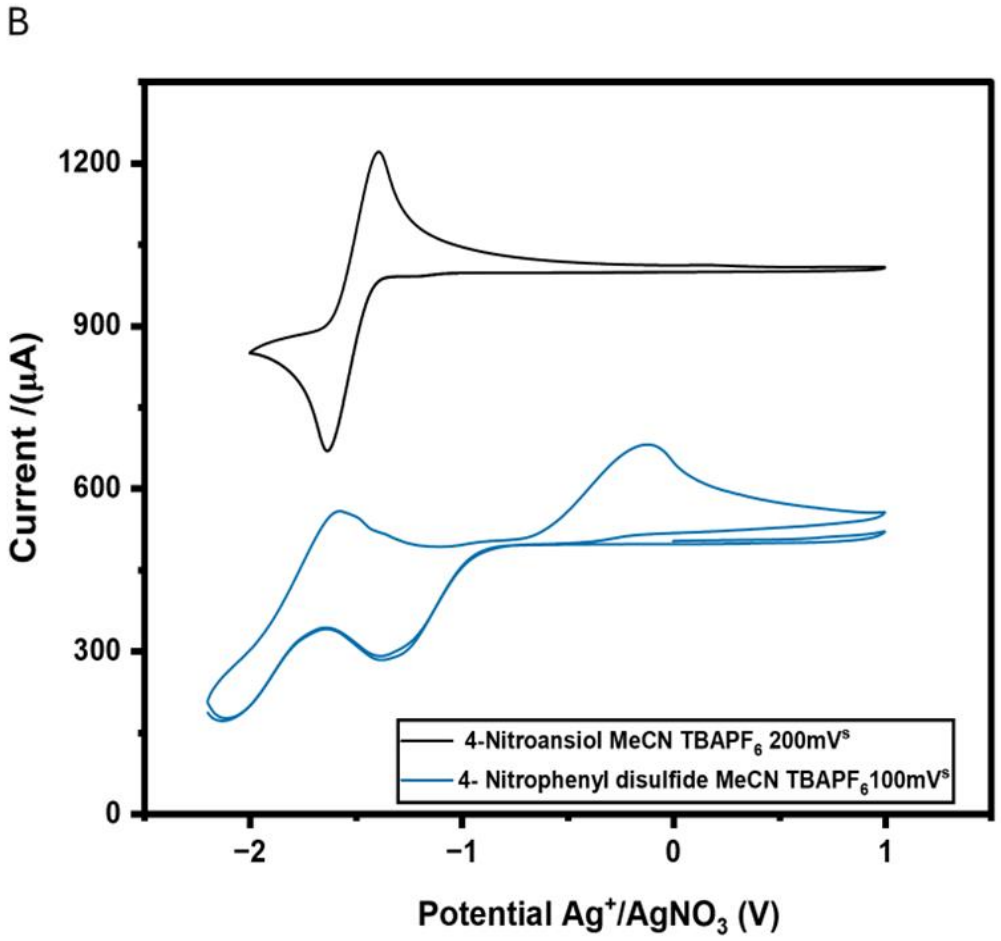

Figure15. (B) 4-nitroanisole and 4-nitrophenyl disulfide as catalytic in MeCN $TBAPF_6$ under N_2.

Figure 15. (B) indicates that 4-nitroanisole displays strong electrochemical activity with sharp redox peaks and significant electron transfer indicating a more straightforward redox process. where the nitro group is attached to an aromatic ring with methoxy group the CV reveals well defined redox peaks indicating a reversible redox process. The electron donating methoxy group stabilises the nitro group promoting faster electron transfer 4-nitrophenyl disulfide on the other hand exhibits broader shows broader peaks suggesting more complex or less reversible redox processes due to the electron withdrawing effect of the disulfide linkage. Both compounds show reversible behaviour but 4-nitroanisole exhibits much stronger and clearer redox activity.

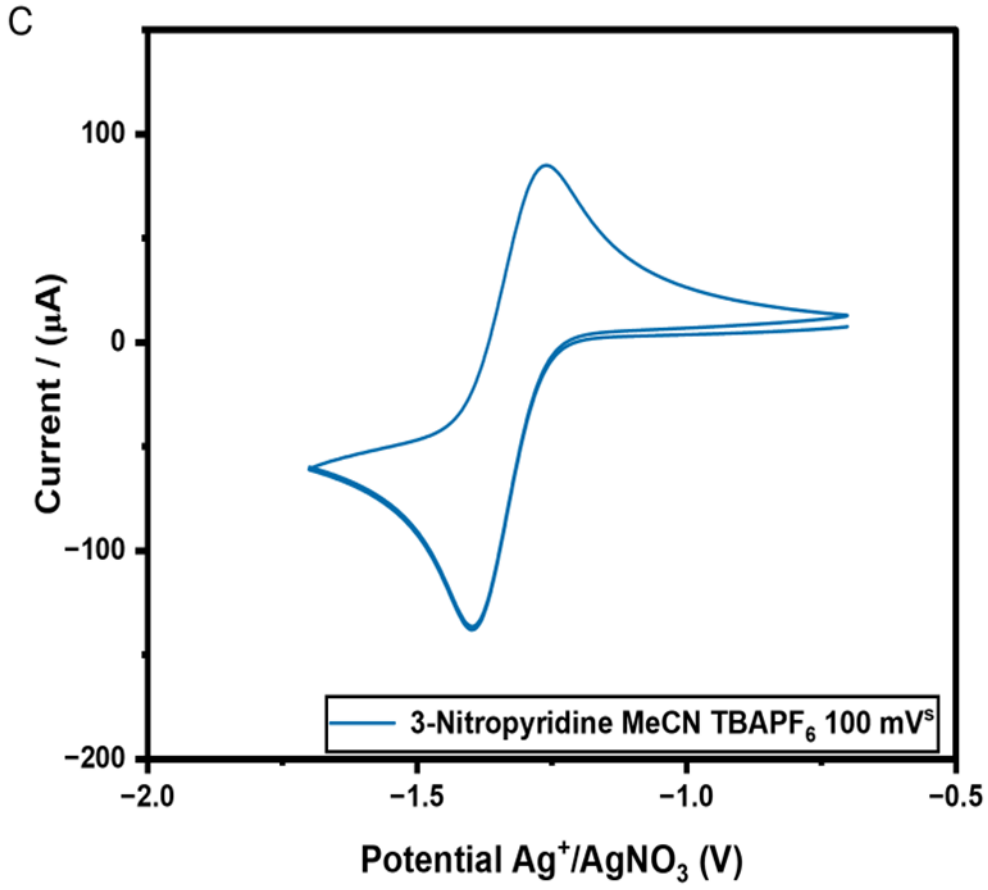

Figure16. (C) 3-nitrpyridine as catalytic in MeCN $TBAPF_6$ under N_2.

Figure 16. (C) shows 3-nitropyridine as a highly reversible redox process with significant electron transfer. The close symmetric redox peaks and minimal peak separation indicate fast electron transfer with very few structural changes making it a good example of a reversible electrochemical process. likely influenced by the stabilising effect of the pyridine ring which facilitates electron transfer.

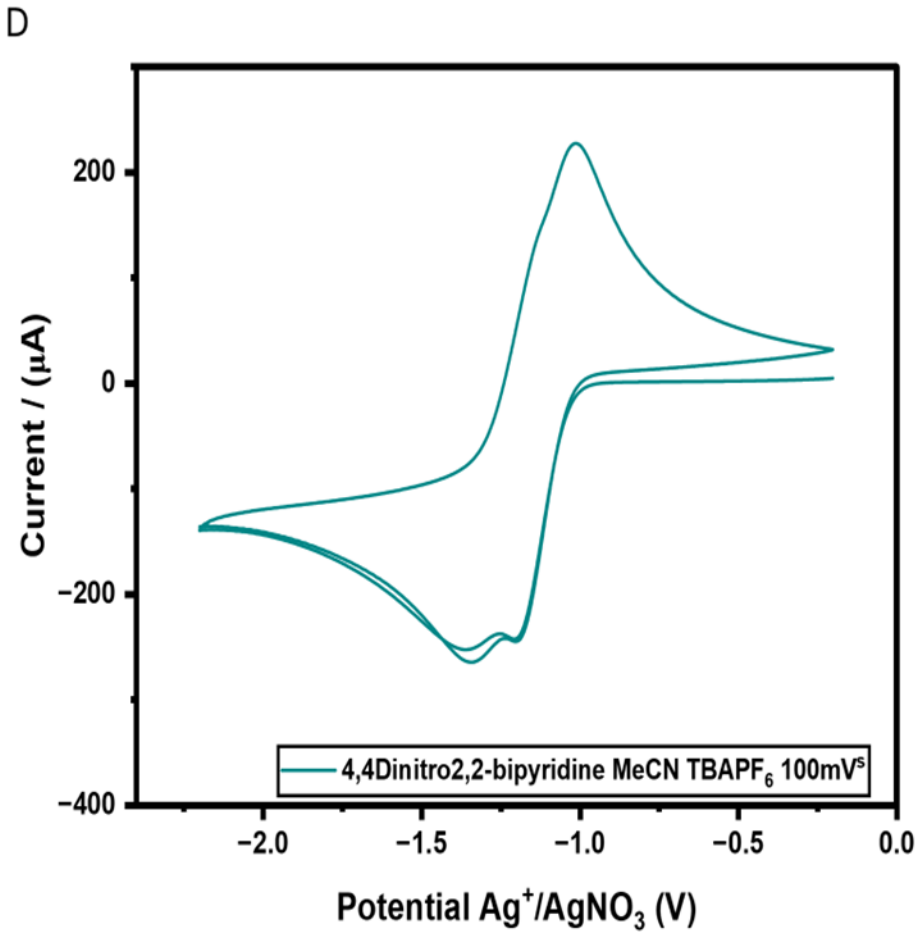

Figure17. (D) 4,4'-Dinitro-2,2'-bipyridine as catalytic in MeCN $TBAPF_6$ under N_2.

In figure 17. (D) show that 4,4'-dinitro-2,2'-bipyridine displays substantial electron transfer and a reversible redox process characterized by well-defined peaks and minimal peak separation. The significant electron transfer is likely driven by the combined effect of the two pyridine rings which stabilize the intermediates and the two nitro groups which increase the molecule's reactivity. Together, these functional groups enhance both the redox behaviour and the reversibility of the process.

Overall, Aromatic and aliphatic nitro compounds differ significantly in their electrochemical behaviour. Aromatic nitro compounds such as, nitrobenzene, 4-nitroanisole, and 3-nitropyridine, have conjugated systems that stabilize intermediate species during redox reactions leading to good reversibility efficient electron transfer and well-defined redox peaks. In contrast, aliphatic nitro compounds such as 1-nitropropane lack this stabilising effect resulting in poorer reversibility weaker redox peaks and significant structural changes during electron transfer. Based on this trend, aliphatic nitro compounds were excluded from further studies while the focus shifted to aromatic nitro compounds which provide more stable and predictable electrochemical behaviour duo to their enhanced electron withdrawing effects and intermediate stability.

6.1.3. Ferrocene (C_{10} H_{10} Fe):

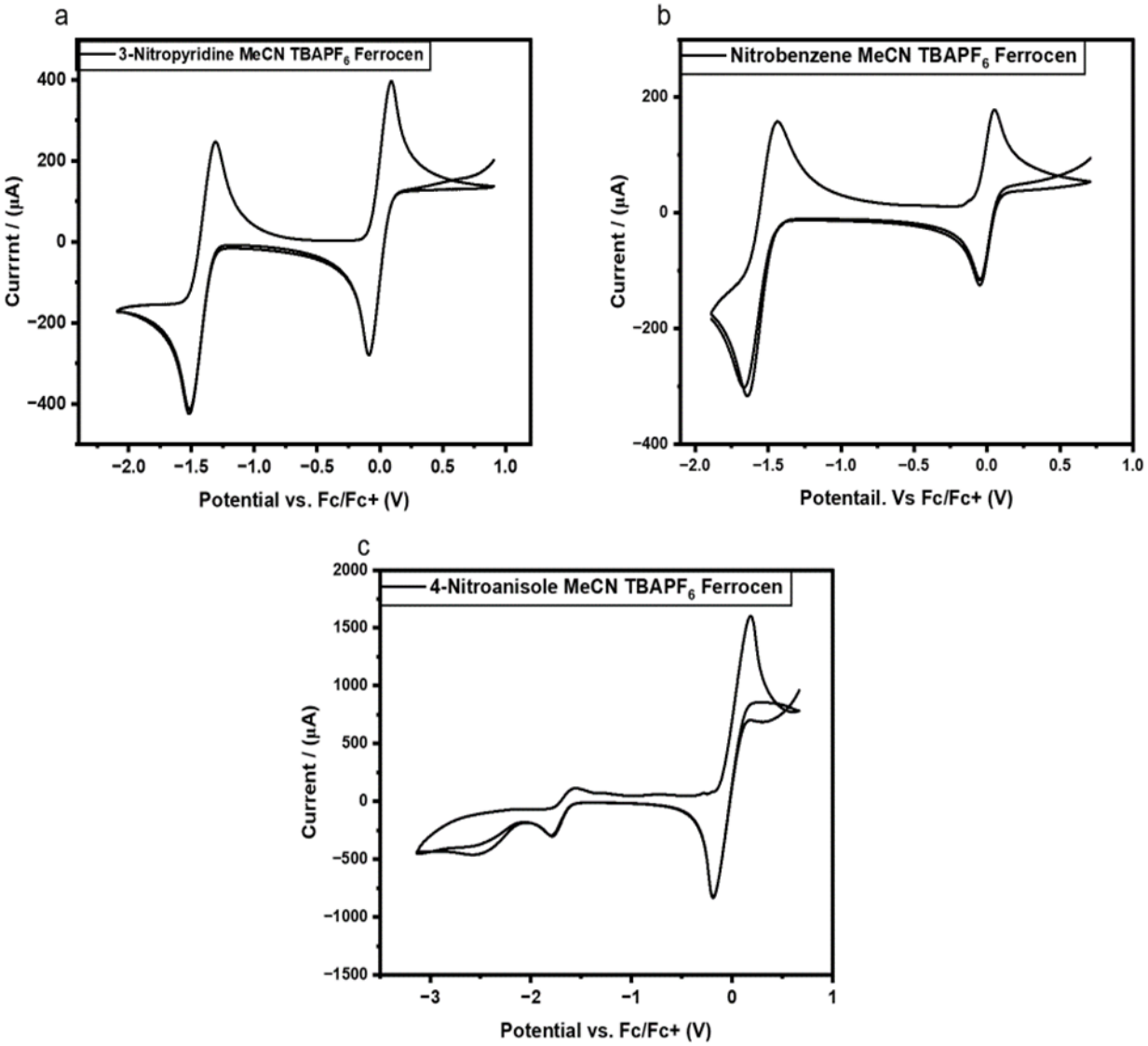

Figure18. CV 3-nitropyridine, Nitrobenzene, and 4-nitro anisole VS Fc/Fc+ (V).

	compound	E_{pa} (V)	E_{pc} (V)	E_{half} (V)	ΔEp (V)
1	3-Nitropyridine	-1.31	-1.52	-1.42	0.21
2	Nitrobenzene	-1.43	-1.64	-1.52	0.21
3	4-Nitroanisole	-1.56	-1.79	-1.68	0.23

This table shows the redox peak data including the anodic peak potentials (E_{pa}) cathodic peak potentials half-wave potentials (E_{half}) and peak-to-peak separation (ΔEp).

For the equation to calculate the half-wave potential (E_half):

$$E_{half} = \frac{(E_{pa} + E_{pc})}{2}$$

And for the peak-to-peak separation (∆Ep):

$$\Delta Ep = Epa - Epc$$

These equations are essential for analysing the reversibility of the redox processes.

A small ∆Ep indicates a more reversible process while larger values suggest less reversible behaviour.

To analyse the three cyclic voltammograms of 3-nitropyridine, nitrobenzene, and 4-nitroanisole (Figures a, b, and c) ferrocene was used as the internal standard to ensure consistency in potential measurements. The cyclic voltammograms were plotted with the potential range aligned to ferrocene's redox peak allowing direct comparison between the different compounds.

3-Nitropyridine (a) The cyclic voltammogram of 3-nitropyridine shows a redox process with an anodic peak (E_{-pa}) at -1.31 V and a cathodic peak (E_{-pc}) at -1.52 V, giving a half-wave potential (E_{-half}) of -1.42 V the peak-to-peak separation (ΔEp) of 0.21 V indicates reversibility.
Nitrobenzene (b) shows similar redox behavior with an anodic peak at -1.43 V and a cathodic peak at -1.64 V resulting in an E_{-half} of -1.52 V. The ΔEp of 0.21 V also indicates reversible behaviour slightly more reversible than 3-nitropyridine.
4-Nitroanisole (c) displays more pronounced redox activity with an anodic peak at -1.56 V and a cathodic peak at -1.79 V giving an E_{-half} of -1.68 V. The ΔEp of 0.23 V suggests reversibility with a higher current indicating more efficient electron transfer.

Overall, using ferrocene as a reference provides a reliable potential scale and the comparison between the compounds demonstrates the different electrochemical behaviours of the nitroaromatic systems. The relatively small ΔEp values across all three compounds suggest reversible behaviour characteristic of nitro group reduction.

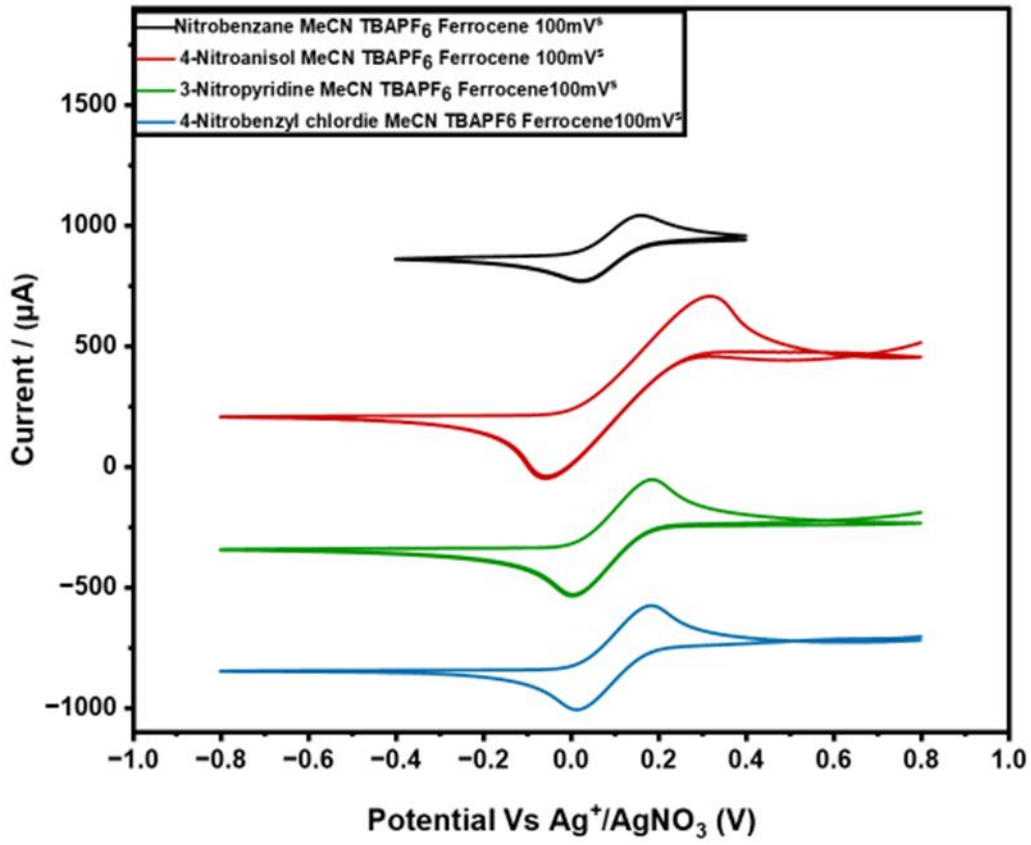

Figure 19. CV for the Ferrocene reduction and oxidisation peaks.

To ensure the accuracy of the results ferrocene was used as an internal reference in the CV experiments to assess the reversibility of the nitro group's redox behaviour.[51] Ferrocene known for its well-defined and reversible redox properties provided a stable reference point for the potential measurements. The inclusion of ferrocene a well-characterised redox couple provided a standard against which the electrochemical properties of the nitroaromatic compounds could be evaluated. By comparing the observed redox potentials and peak separations of the nitro groups to those of the ferrocene/ferrocenium (Fc/Fc+) couple it was possible to determine the degree of reversibility in the nitro reduction and oxidation processes.[58] This internal referencing approach is a common practice in electrochemical studies as it helps to minimize the effects of experimental variables such as electrode kinetics and enables more

meaningful comparisons between different systems. [59] With ferrocene as the reference compounds such as 4-nitroanisol and 3-nitropyridine and nitrobenzene shows clear reversible peaks indicating stable electron transfer. The use of ferrocene enabled a more accurate comparison of the redox behaviour across the compounds highlighting the differences in reversibility among the aromatic nitro compounds.

6.1.4. Aromatic catalysis with aqueous electrolyte under N_2 and CO_2:

CV experiments were conducted to compare the redox behaviour of pyridine, 2-nitropyridine, 3-nitropyridine, nitrobenzene,4-nitroanisole, 4-nitrobenzyl chloride, and 4,4-Dinitro-2,2-bipyridine in bicarbonate buffer ($KHCO_3$) with H_2O under different gas environments N_2 (black curve) and CO_2 (red curve) at scan rate of 20mV/^{s}.

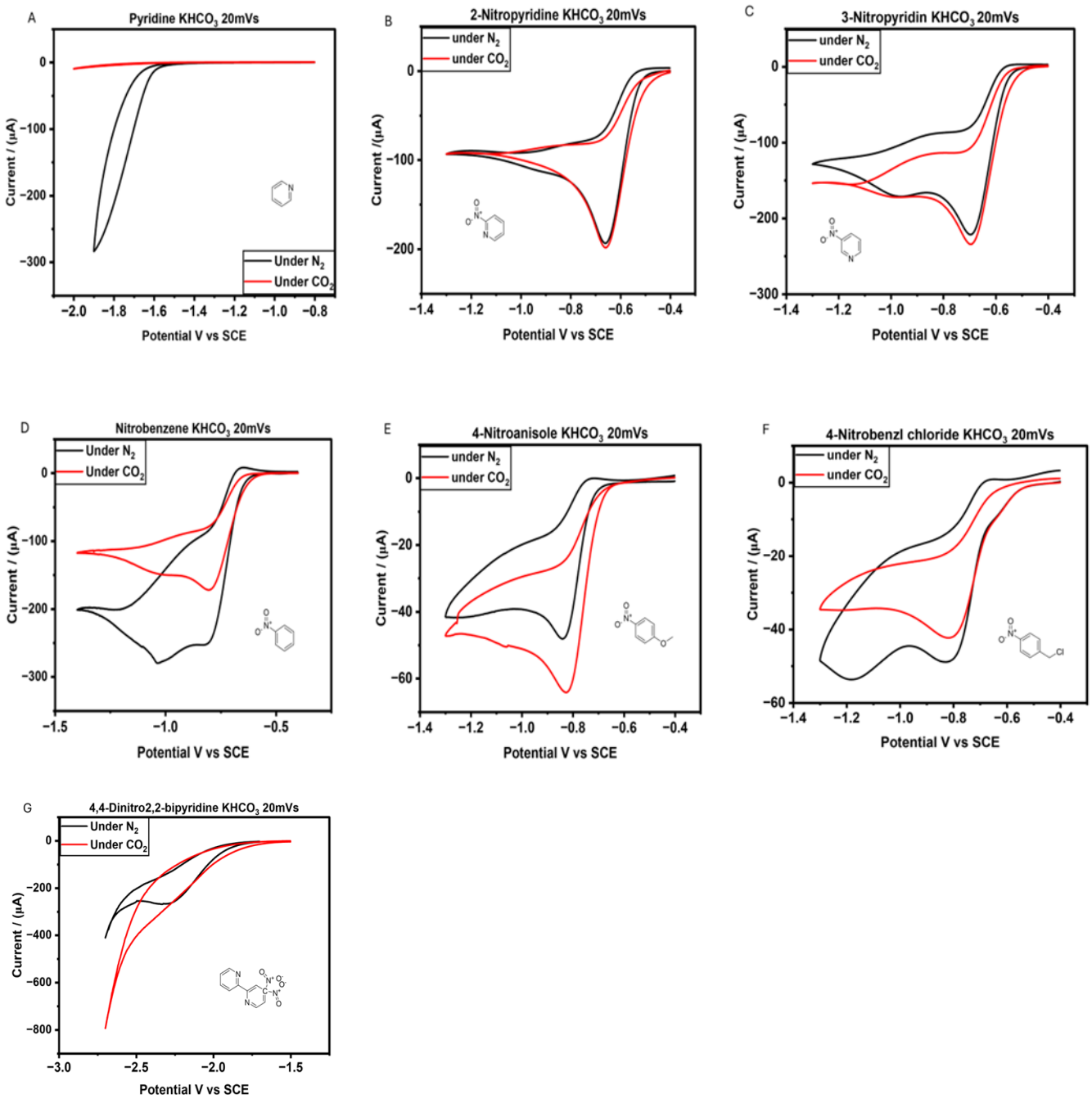

Figure 20. CV for various Nitro group compounds under N_2, CO_2 in $KHCO_3$ as electrolyte with H_2O.

Pyridine (A): The CV indicates a large increase in activity under both N_2 and CO_2 atmospheres. This suggest that pyridine may be promising candidate for use in electrocatalytic CO_2 reduction processes.[60] Studies such as Peroff et al. (2016) indicate that the presence of CO_2 alters the reaction pathway for pyridinium. In particular CO_2 may facilitate hydrogen evolution or engage in alternative reactions making certain intermediates less detectable in electrochemical systems.[61] Similarly, research by Keith and Carter(2013) highlights that the pyridinium electrochemical behaviour can change depending on whether CO_2 present that's mean CO_2 could be interacting with pyridinium in a way that changes the reduction potential or leads to different products such as hydrogen evolution effectively masking or altering the expected electrochemical response.[62] This may explain why Figure (A) shows a peak under N_2 but not under CO_2 as CO_2 may shift the reaction mechanism away from the formation of detectable pyridinium intermediates.

2-nitropyiridne (B), displays clearly defined redox peaks which include a reduction peak at around -0.6 V and a matching oxidation peak under both N_2 and CO_2 indicating substantial electrochemical activity. The peak separation is larger compared to pyridine, suggesting a more quasi-reversible behaviour.

3-nitropyridine (C), similar to 2-nitropyridine catalysts showed apparent redox activity with a larger peak separation increased reduction capacity in both N_2, and CO_2 conditions. This observation would suggest the nitro group demonstrates higher reactivity when interacting with CO_2.

Nitrobenzene (D), a well-defined redox peak is observed with reduction occurring at approximately -1.0V. the presence of CO_2 slightly enhances the reduction current suggesting a possible catalytic influence of CO_2 on the redox reactivity.

4-nitroanisole (E), the CV under CO_2 exhibits a much larger reduction peak compared to the peak under N_2 this suggest that the 4-nitroanisole has a higher affinity and activity towards the electrochemical reduction of CO_2.

4-nitrobenzyl chloride (F), the CV shows well defined redox peak under N_2 and less under CO_2.

4,4-Dinitro-2,2-bipyridine (G) The CV exhibits the smallest peak separation between reduction and oxidation under both N_2 and CO_2.

Overall, under CO_2 conditions, the red curves show higher cathodic currents than in N_2 conditions, especially in the nitro groups such as 3-nitropyridine, and 4-nitroanisole based on the observation these compounds may be the most promising for energy efficient electrochemical CO_2 reduction among the other materials. This suggests that CO_2 may be interacting with the reduced species or influencing the redox processes which stabilising the intermediates and promoting further reduction. Despite, the nitro group (-NO_2) is present in all compounds in the CV experiments which is evidenced by the slight similarity in the reduction peaks. This group endures a similar electrochemical reduction process. This typically entails a two-electron transfer to generate a nitroso intermediate. Furthermore, the data obtained from CV indicate that the nitro compounds have irreversible characteristics. This mainly due to the reduction of the nitro group (-ON_2) which leads in the formation of unstable intermediates such as hydroxylamine's the intermediates undergo additional chemical reactions that slow the reverse oxidation process therefore adding to the irreversibility of the reaction. The use of potassium bicarbonate ($KHCO_3$) in the electrolyte enhances this trend. The slightly alkaline environment provided by $KHCO_3$ may stabilise the reduction intermediates but also promotes side reaction such as protonation or interactions with bicarbonate ions which prevent a complete oxidation response.[63] These side reactions result in the loss of reversibility in the redox cycles as observed in the CV graphs. The cyclic voltammograms show that the nitro compounds don't have the reversible redox behaviour needed for efficient CO_2 reduction. The wide separation between peaks means higher energy use and costs. Improvements in design and catalysts are necessary to make the process more efficient and cost-effective. Therefore, the presence of unstable intermediates and the chemical environment generated by $KHCO_3$ leads to the overall irreversibility of the redox reaction in these experiments.

6.1.5. Aromatic catalysis with non-aqueous electrolyte under N_2 and CO_2:

These CV graphs illustrate the electrochemical behaviours of seven compounds Pyridine,2-nitropyridine,3-nitropyridine, nitrobenzene,4-nitroanisole,4-nitrobenzyl chloride, and 4,4-dinitro2,2-bipyridine under two gas environments nitrogen (N_2, black) and carbon dioxide (CO_2, red). The experiments were conducted in MeCN with $TBAPF_6$ at a scan rate of 100 $mV/^s$.

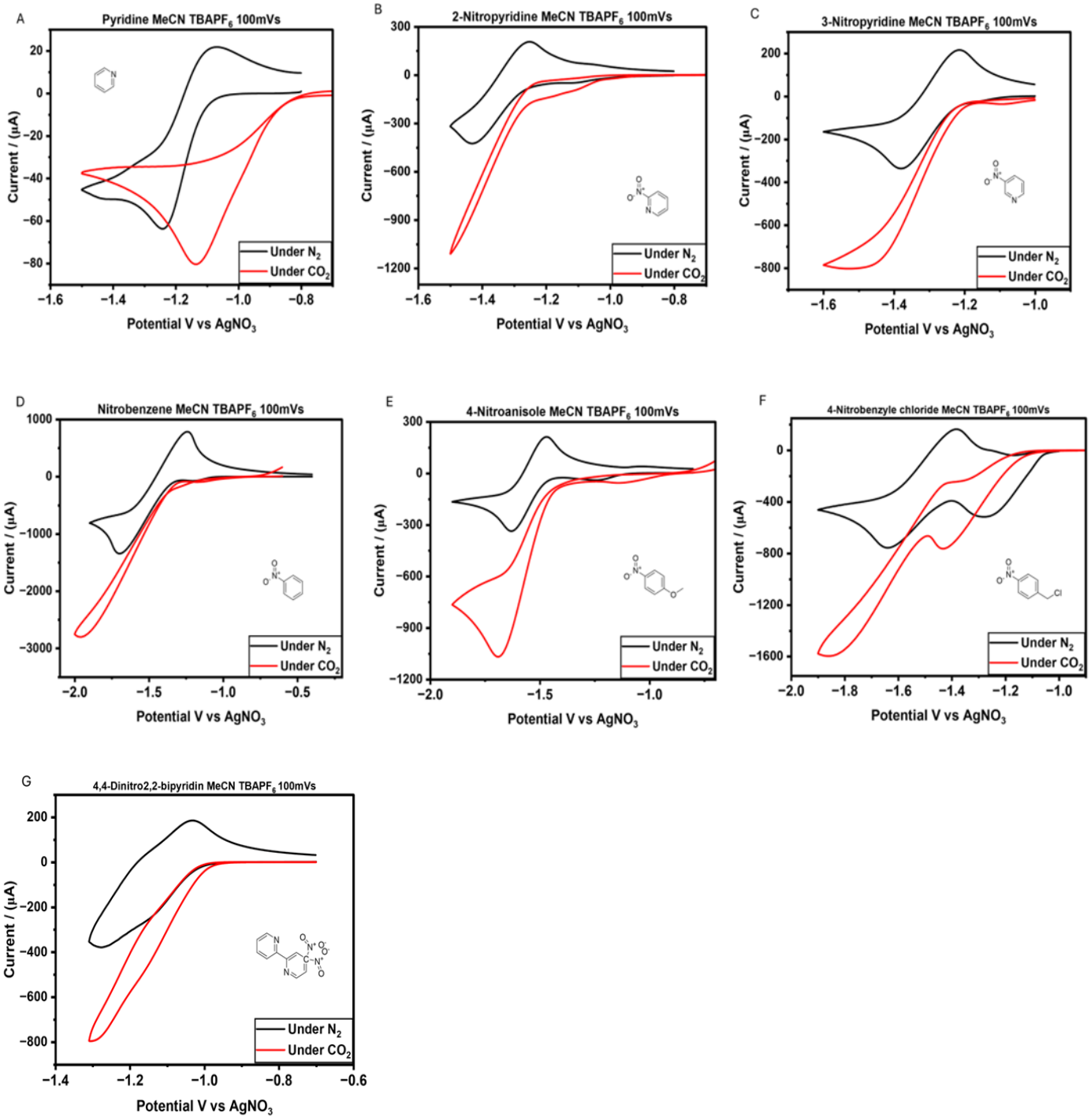

Figure 21. CV for various Nitro group compounds under N_2, CO_2 in MeCN TBAPF6 as electrolyte.

Pyridine (A) shows an increased reduction current under the CO_2 atmosphere compared to the N_2 atmosphere. The increase, though present is not as high as some of the other nitro-containing compounds. This suggests pyridine has some selectivity towards CO_2 reduction but its activity is relatively lower compared to the nitro-substituted derivatives.

2-Nitropyridine (B) and 3-Nitropyridine (C) exhibit apparent reduction and oxidation peaks under NO_2 with enhanced cathodic current under CO_2 increase the reduction peak indicating that CO_2 promotes the reduction of nitro groups. In 2-nitropyridine, the nitro group at the ortho position exerts a strong electron-withdrawing effect on the nitrogen atom significantly reducing electron density and nucleophilicity. In contrast, 3-nitropyridine features the nitro group at the meta position where the electron-withdrawing effect this allows for better conjugation and results in greater stability compared to 2-nitropyridine. This is also observed in Nitrobenzene (D) and 4-Nitroanisole (E) where the CO_2 environment amplifies the reduction peaks suggesting interaction with reduced nitro species. In nitrobenzene, the nitro group (-NO_2) strongly withdraws electron density from the benzene ring reducing nucleophilicity and making it less reactive toward electrophilic substitution while increasing susceptibility to nucleophilic aromatic substitution. Which also shows strong selectivity for CO_2 reduction although it did not appear the same as the 4-nitroanisole. In 4-nitroanisole, the methoxy group (-OCH_3) at the para position donates electron density creating a push-pull effect with the nitro group. This increases the reactivity of 4-nitroanisole toward electrophilic substitution particularly at positions activated by the methoxy group.[64] For the energy efficiency the 4-nitroanisole this compound shows an exceptionally large increase in reduction current under CO_2 indicating it is highly selective and active towards reducing CO_2. Its ability to facilitate the reduction at lower voltages makes 4-nitroanisole the most energy-efficient option. On the other hand, the 4-Nitrobenzyl chloride (F) Shows an increased reduction current under CO_2 but the magnitude of the increase is less pronounced compared to the other nitro-containing compounds which shows the least improvement in energy efficiency.

4-4'-Dinitro-2-2'-bipyridine (G) displays similarly enhanced reduction under CO_2 suggesting that CO_2 may facilitate electron transfer or stabilise intermediate species across all nitro-containing compounds. By strongly withdrawing electron density from

the bipyridine effects the nitro groups (-NO_2) influence the electronic properties of 4,4'-dinitro-2,2'-bipyridine. As a result, the molecule becomes more electron-deficient stabilising any negative charge during reduction and shifting its reduction potential, facilitating electron acceptance. Due to its electron-deficient nature bipyridines are more likely to interact with reduced CO_2 species during CO_2 reduction. In addition to their ability to undergo reduction under strong conditions the nitro groups also modulate the catalytic activity of the bipyridine.

In all cases the increase in cathodic current under CO_2 points to its potential role in stabilising intermediates promoting further electron transfer and possibly contributing to the formation of new products.

Overall, in these CV experiments, the transfer of electrons primarily occurs during the reduction and oxidation of the compounds' nitro group (-NO_2). When a nitro group is reduced it gains electrons which are transferred to the nitro group typically reducing it to nitroso (-NO_2) or hydroxylamine intermediates.

Under CO_2, this electron transfer is enhanced as seen by the increase in the cathodic current. CO_2 likely interacts with these intermediates stabilising them and promoting further reduction. This interaction increases the overall electron transfer suggesting that CO_2 facilitates the reduction process forming new products. That could be because the reduced nitro group reduces the CO_2. The nitro group can then be reduced again, However, under N_2, these reductions are less pronounced as there is no additional interaction with CO_2 to stabilise the intermediates or promote further electron transfer.

In summary, the presence of CO_2 creates an environment that enhances electron transfer to the nitro groups resulting in more efficient reduction and potentially new products formation due to the interaction between CO_2 and the reduced species. In terms of energy-efficient electrochemical CO_2 reduction 4-nitroanisole is the clear leader in terms of energy-efficient electrochemical CO_2 reduction, followed by nitrobenzene and 2-nitropyridine with the other compounds. In conclusion, the efficiency of CO_2 reduction is significantly influenced by the structure and composition of catalysts, including the incorporation of the functional groups modify the electronic properties and catalytic environment leading to varied interactions with CO_2 molecules.

7. Characterisation NMR:

Nuclear magnetic resonance (NMR) spectroscopy played a central role in the structural characterization of the compounds investigated in this study. The NMR data provided critical insights into the nitro-containing aromatic systems' chemical composition and structural features. Through analysis of the ^{1}H, ^{19}F, and ^{31}P NMR spectra, the experiments confirmed the expected structures of critical compounds, including 2-nitropyridine, 3-nitropyridine, 4-nitroanisole, and nitrobenzene.[65] The proton NMR data revealed characteristic aromatic signals corresponding to the nitroaromatic moieties, while additional peaks from the solvent, supporting electrolyte, and water were also consistently observed. Furthermore, the ^{19}F and ^{31}P NMR spectra verified the presence of the PF_6- counterion derived from the $TBAPF_6$ electrolyte used in the electrochemical experiments.[66]In this research the application of NMR spectroscopy was crucial for confirming the expected chemical structures of the nitroaromatic compounds under investigation. The characteristic signals observed in the proton NMR spectra corresponding to the aromatic protons provided clear evidence of the nitro group substitution patterns. Furthermore, the additional information obtained from heteroatom NMR experiments such as ^{19}F and ^{31}P NMR for the supporting electrolyte enabled a more complete structural validation.[67]By correlating the NMR data with the electrochemical insights gained from cyclic voltammetry, a comprehensive understanding of the nitroaromatic systems and their behaviour could be developed informing the design of future applications and reactions.

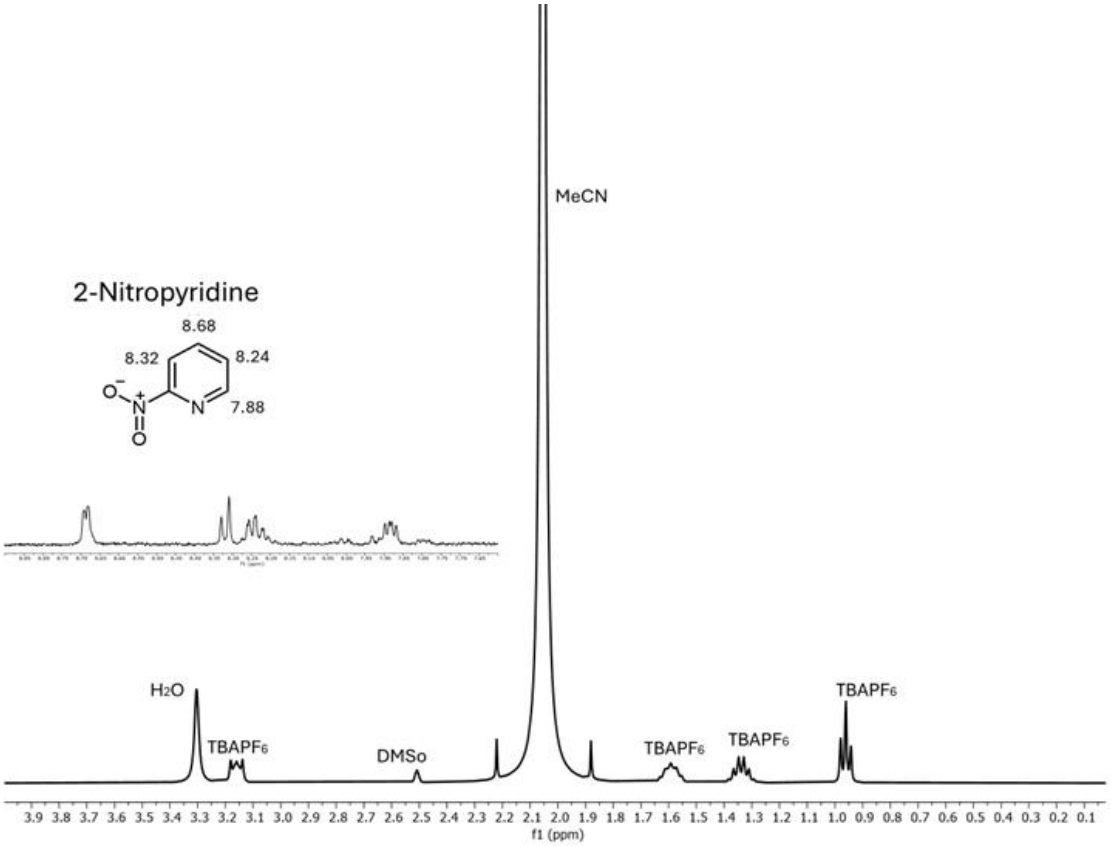

Figure 22. NMR spectrum 2-nitropyridine in DMSO-6.

The NMR spectrum of 2-nitropyridine shows aromatic proton peaks between 7.88 ppm and 8.68 ppm, corresponding to the protons on the pyridine ring. The peak at 2.1 ppm is attributed to the solvent MeCN. Peaks corresponding to the supporting electrolyte $TBAPF_6$ appear between 1.4 ppm and 1.6 ppm with an additional small peak near 0.9 ppm. A water signal is also visible at 3.4 ppm. This spectrum confirms the presence and structure of 2-nitropyridine, MeCN, and $TBAPF_6$ in the solution.

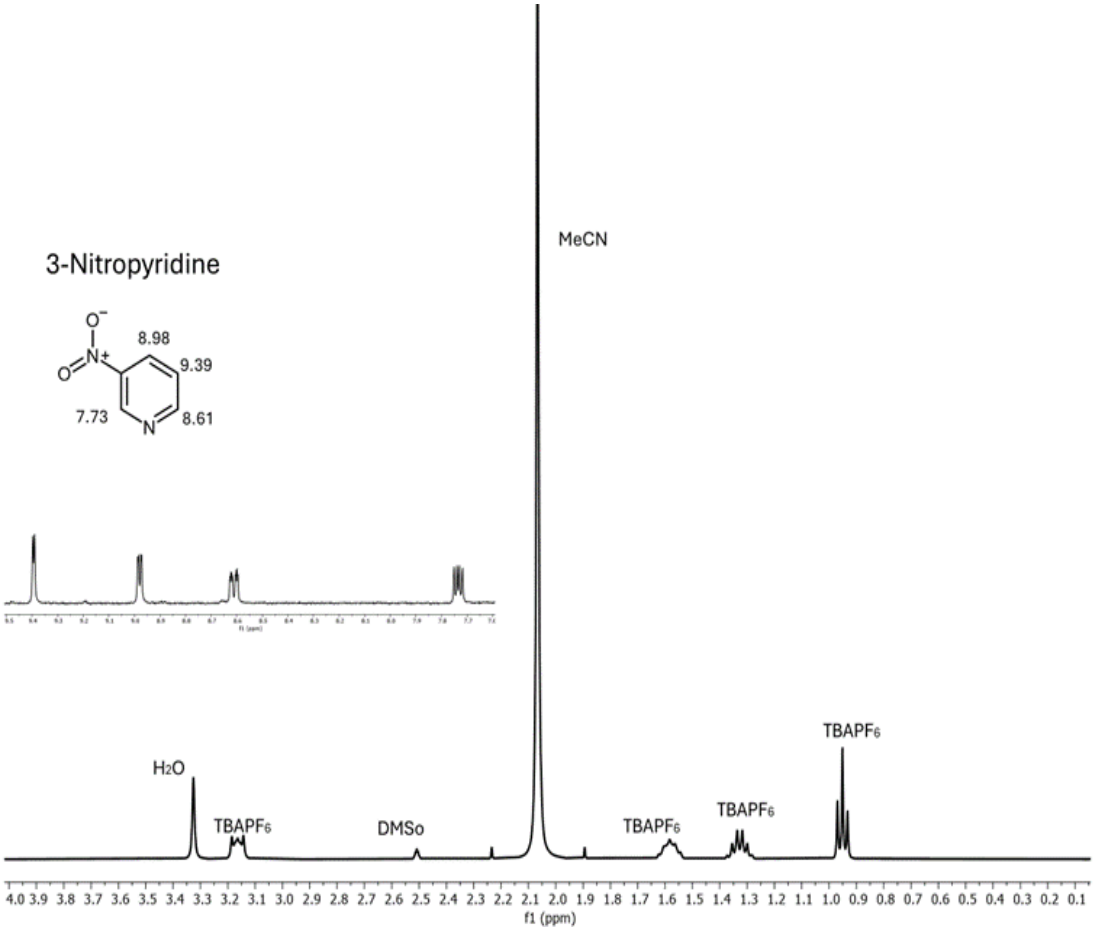

Figure 23. NMR spectrum 3-nitropyridine in DMSO-6.

The NMR spectrum for 3-nitropyridine exhibits distinct aromatic proton peaks between 7.73 ppm and 9.39 ppm corresponding to the protons on the pyridine ring. The dominant peak at 2.1 ppm is attributed to MeCN the solvent used. The presence of $TBAPF_6$ the supporting electrolyte is confirmed by peaks around 1.4 to 1.6 ppm and a smaller peak at 0.9 ppm. Additionally, a water peak is visible at around 3.4 ppm. This spectrum provides clear confirmation of the 3-nitropyridine structure and the solution composition.

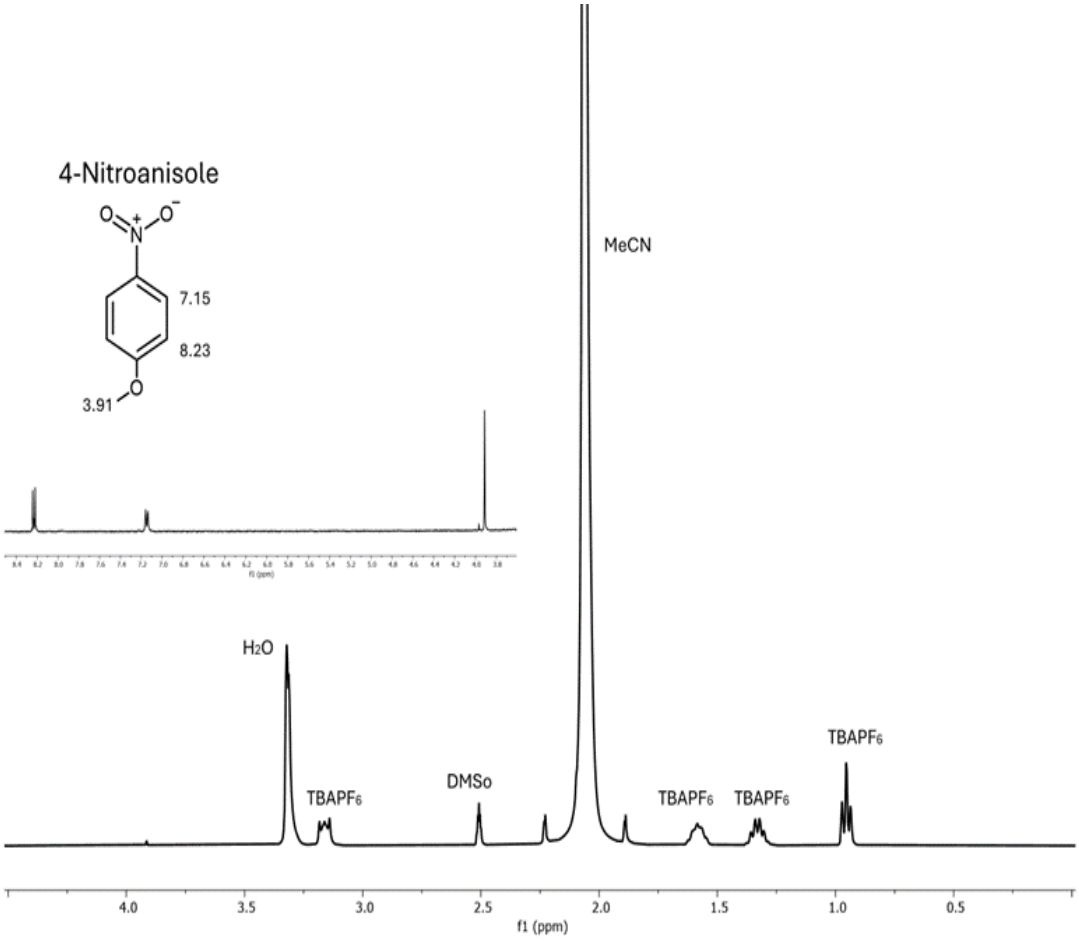

Figure 24. NMR spectrum 4-nitroanisole in DMSO-6.

The NMR spectrum of 4-nitroanisole shows characteristic aromatic proton signals, with peaks at 7.15 ppm and 8.23 ppm, corresponding to the protons on the aromatic ring. The peak at 3.91 ppm is attributed to the methoxy (-OCH_3) group attached to the aromatic ring. The solvent MeCN represents the peak around 2.1 ppm. Peaks for $TBAPF_6$ are observed between 1.4 and 1.6 ppm with an additional peak near 0.9 ppm. A small peak for water appears around 3.4 ppm. This spectrum confirms the identity and composition of the solution.

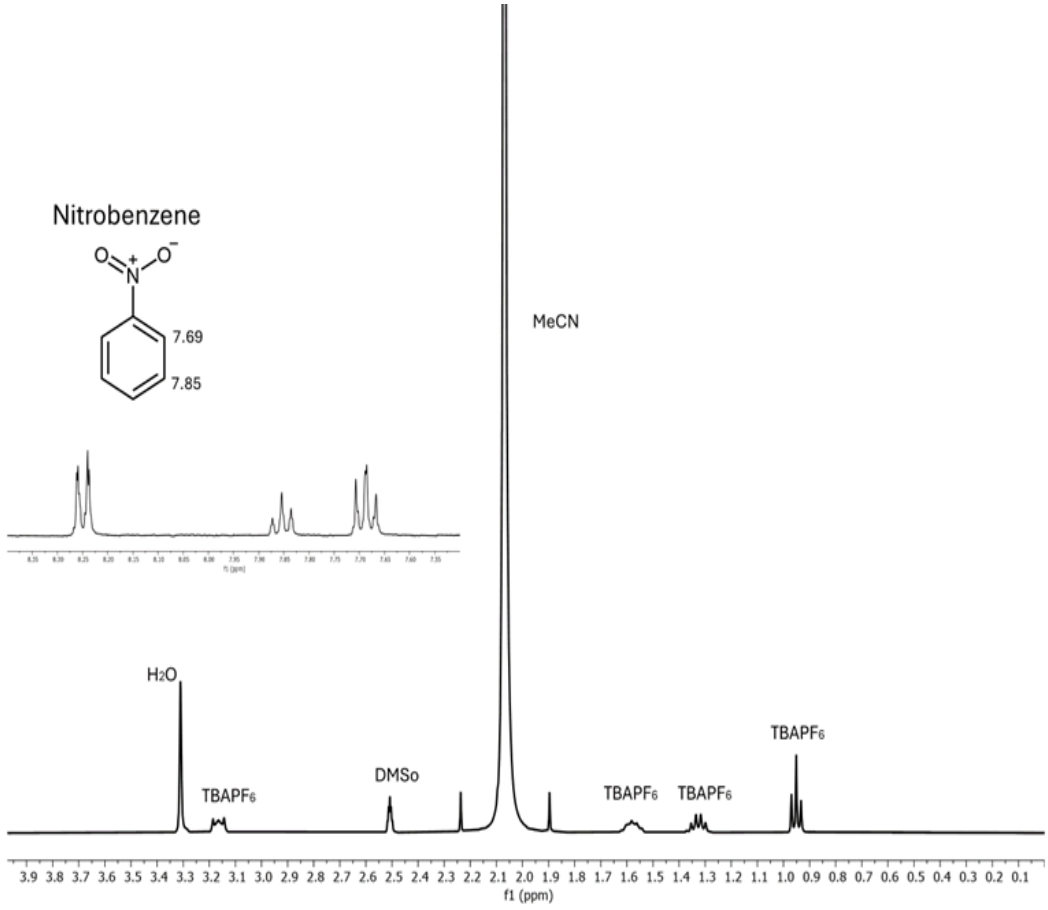

Figure 25. NMR spectrum nitrobenzene in DMSO-6**.**

The NMR spectrum for nitrobenzene shows aromatic proton peaks at 7.69 ppm and 7.85 ppm characteristic of the protons on the benzene ring. The large peak at 2.1 ppm corresponds to MeCN which is the solvent used in the sample. Peaks for $TBAPF_6$ are observed between 1.4 and 1.6 ppm and at 0.9 ppm along with a water signal around 3.4 ppm. Additionally, a peak at 2.6 ppm corresponds to DMSO. This spectrum confirms the presence of nitrobenzene, MeCN, and $TBAPF_6$ in the solution.

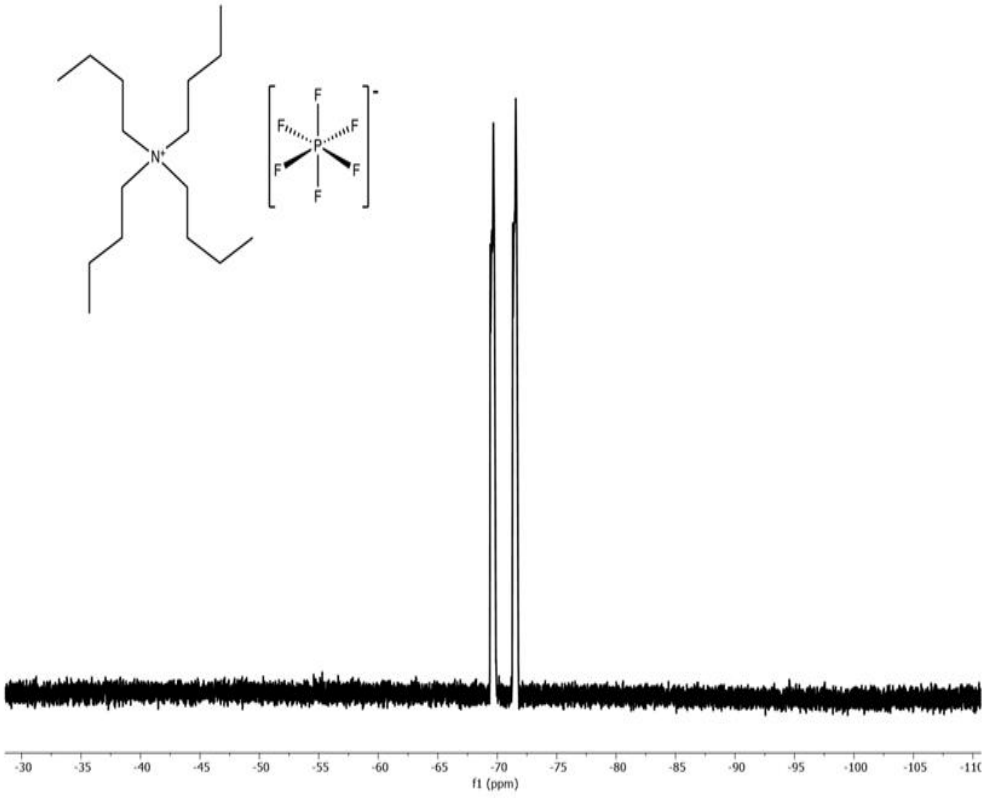

Figure 26. NMR a ^{19}F NMR for the fluorinated spectrum of the PF_6^- anion.

This spectrum appears to be a ^{19}F NMR for the fluorinated component of the $TBAPF_6$ salt, specifically the PF_6^- (hexafluorophosphate**)** anion. The doublet at approximately **-**70 ppm corresponds to the six equivalent fluorine atoms attached to the phosphorus atom in the PF_6^- ion. The doublet pattern arises due to the spin-spin coupling between the fluorine atoms and the phosphorus nucleus (^{19}F-^{31}P coupling), a characteristic feature of PF_6^- in NMR spectroscopy. This confirms the presence of the $TBAPF_6$ salt in the sample.

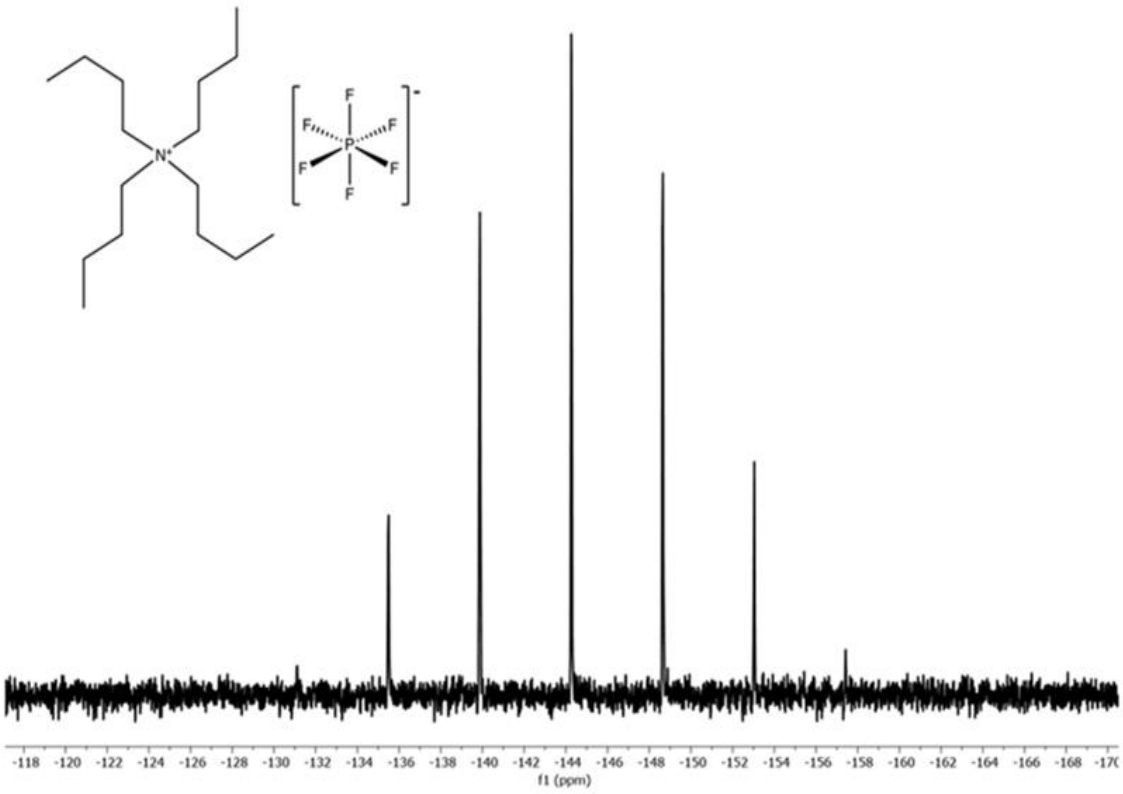

Figure 27. A ^{31}P NMR of the PF_6^- anion.

This spectrum is a ^{31}P NMR of the PF_6^- anion from TBAPF6. The signal appears in the range of -140 to -150 ppm which is characteristic of phosphorus in the PF_6^- ion. The splitting pattern is due to the coupling between the phosphorus atom ^{31}P and the six equivalent fluorine atoms ^{19}F in the anion producing typical multiple signals. The distinct peak at this chemical shift confirms the presence of the hexafluorophosphate ion in the sample as expected for TBAPF6.

8. Conclusion:

In conclusion, this work explored the electrochemical behaviour and structural analysis of nitro containing aromatic compounds focusing on their interactions under different conditions particularly in the presence of CO_2.

Cyclic voltammetry experiments demonstrated enhanced reduction currents for these nitroaromatic compounds under CO_2 atmospheres. This suggests that CO_2 plays a vital role in the redox processes potentially leading to the formation of new products.

NMR spectroscopy was a crucial analytical technique used to confirm the structures of specific compounds including 2-nitropyridine, 3-nitropyridine, 4-nitroanisole, and nitrobenzene. The NMR data also verified the presence of $TBAPF_6$ as the supporting electrolyte used in these electrochemical studies.

Overall, the findings from this work contribute to a deeper fundamental understanding of nitro group reduction mechanisms and the influence of CO_2 on these redox processes involving nitroaromatic systems. The comprehensive structural characterization provides an essential context for interpreting the electrochemical behaviour. This knowledge can inform the development of new reactions and applications involving nitro-containing aromatic compounds.

9. Future work:

Exploring could involve the use of Gas Chromatography (GC) coupled with Differential Electrochemical Mass Spectrometry (DEMS) to analyse further and identify the electrochemical reduction products formed during cyclic voltammetry (CV) experiments under CO_2. This would provide more accurate insights into the new species formed. Additionally, further NMR studies on the isolated products could be conducted to characterise the molecular structures of these new products enabling a deeper understanding of the mechanistic pathways involved in the reduction of nitroaromatic compounds in the presence of CO_2.

Bibliography:

(1) Anwar, M. N.; Iftikhar, M.; Khush Bakhat, B.; Sohail, N. F.; Baqar, M.; Yasir, A.; Nizami, A. S. Sources of Carbon Dioxide and Environmental Issues. In *Sustainable Agriculture Reviews 37*; Inamuddin, Asiri, A. M., Lichtfouse, E., Eds.; Sustainable Agriculture Reviews; Springer International Publishing: Cham, 2019; Vol. 37, pp 13–36. https://doi.org/10.1007/978-3-030-29298-0_2.

(2) Frame, D. J.; Harrington, L. J.; Fuglestvedt, J. S.; Millar, R. J.; Joshi, M. M.; Caney, S. Emissions and Emergence: A New Index Comparing Relative Contributions to Climate Change with Relative Climatic Consequences. *Environ. Res. Lett.* **2019**, *14* (8), 084009. https://doi.org/10.1088/1748-9326/ab27fc.

(3) Chen, J.; Li, X.; Martel, J.-L.; Brissette, F. P.; Zhang, X. J.; Frei, A. Relative Importance of Internal Climate Variability versus Anthropogenic Climate Change in Global Climate Change. *Journal of Climate* **2021**, *34* (2), 465–478. https://doi.org/10.1175/JCLI-D-20-0424.1.

(4) Jiang, X.; Guan, D. Determinants of Global CO2 Emissions Growth. *Applied Energy* **2016**, *184*, 1132–1141. https://doi.org/10.1016/j.apenergy.2016.06.142.

(5) Solomon, S.; Plattner, G.-K.; Knutti, R.; Friedlingstein, P. Irreversible Climate Change Due to Carbon Dioxide Emissions. *Proc. Natl. Acad. Sci. U.S.A.* **2009**, *106* (6), 1704–1709. https://doi.org/10.1073/pnas.0812721106.

(6) Fearnside, P. M. Deforestation in Brazilian Amazonia: History, Rates, and Consequences. *Conservation Biology* **2005**, *19* (3), 680–688. https://doi.org/10.1111/j.1523-1739.2005.00697.x.

(7) Quadrelli, R.; Peterson, S. The Energy–Climate Challenge: Recent Trends in CO2 Emissions from Fuel Combustion. *Energy Policy* **2007**, *35* (11), 5938–5952. https://doi.org/10.1016/j.enpol.2007.07.001.

(8) Wang, J.; Feng, L.; Tang, X.; Bentley, Y.; Höök, M. The Implications of Fossil Fuel Supply Constraints on Climate Change Projections: A Supply-Side Analysis. *Futures* **2017**, *86*, 58–72. https://doi.org/10.1016/j.futures.2016.04.007.

(9) Panwar, N. L.; Kaushik, S. C.; Kothari, S. Role of Renewable Energy Sources in Environmental Protection: A Review. *Renewable and Sustainable Energy Reviews* **2011**, *15* (3), 1513–1524. https://doi.org/10.1016/j.rser.2010.11.037.

(10) Hong, W. Y. A Techno-Economic Review on Carbon Capture, Utilisation and Storage Systems for Achieving a Net-Zero CO2 Emissions Future. *Carbon Capture Science & Technology* **2022**, *3*, 100044. https://doi.org/10.1016/j.ccst.2022.100044.

(11) Lin, Q.; Zhang, X.; Wang, T.; Zheng, C.; Gao, X. Technical Perspective of Carbon Capture, Utilization, and Storage. *Engineering* **2022**, *14*, 27–32. https://doi.org/10.1016/j.eng.2021.12.013.

(12) Schafer, A. G.; Blakey, S. B. Ir-Catalyzed Enantioselective Group Transfer Reactions. *Chem. Soc. Rev.* **2015**, *44* (17), 5969–5980. https://doi.org/10.1039/C5CS00354G.

(13) Zhu, D. D.; Liu, J. L.; Qiao, S. Z. Recent Advances in Inorganic Heterogeneous Electrocatalysts for Reduction of Carbon Dioxide. *Advanced Materials* **2016**, *28* (18), 3423–3452. https://doi.org/10.1002/adma.201504766.

(14) Habisreutinger, S. N.; Schmidt-Mende, L.; Stolarczyk, J. K. Photocatalytic Reduction of CO_2 on TiO_2 and Other Semiconductors. *Angew Chem Int Ed* **2013**, *52* (29), 7372–7408. https://doi.org/10.1002/anie.201207199.
(15) Grodkowski, J.; Neta, P. Copper-Catalyzed Radiolytic Reduction of CO_2 to CO in Aqueous Solutions. *J. Phys. Chem. B* **2001**, *105* (21), 4967–4972. https://doi.org/10.1021/jp004567d.
(16) Chantiwas, R.; Park, S.; Soper, S. A.; Kim, B. C.; Takayama, S.; Sunkara, V.; Hwang, H.; Cho, Y.-K. Flexible Fabrication and Applications of Polymer Nanochannels and Nanoslits. *Chem. Soc. Rev.* **2011**, *40* (7), 3677. https://doi.org/10.1039/c0cs00138d.
(17) Nitopi, S.; Bertheussen, E.; Scott, S. B.; Liu, X.; Engstfeld, A. K.; Horch, S.; Seger, B.; Stephens, I. E. L.; Chan, K.; Hahn, C.; Nørskov, J. K.; Jaramillo, T. F.; Chorkendorff, I. Progress and Perspectives of Electrochemical CO_2 Reduction on Copper in Aqueous Electrolyte. *Chem. Rev.* **2019**, *119* (12), 7610–7672. https://doi.org/10.1021/acs.chemrev.8b00705.
(18) He, H.; Jagvaral, Y. Electrochemical Reduction of CO_2 on Graphene Supported Transition Metals – towards Single Atom Catalysts. *Phys. Chem. Chem. Phys.* **2017**, *19* (18), 11436–11446. https://doi.org/10.1039/C7CP00915A.
(19) Kuhl, K. P.; Cave, E. R.; Abram, D. N.; Jaramillo, T. F. New Insights into the Electrochemical Reduction of Carbon Dioxide on Metallic Copper Surfaces. *Energy Environ. Sci.* **2012**, *5* (5), 7050. https://doi.org/10.1039/c2ee21234j.
(20) Qiao, J.; Liu, Y.; Hong, F.; Zhang, J. A Review of Catalysts for the Electroreduction of Carbon Dioxide to Produce Low-Carbon Fuels. *Chem. Soc. Rev.* **2014**, *43* (2), 631–675. https://doi.org/10.1039/C3CS60323G.
(21) Jouny, M.; Luc, W.; Jiao, F. General Techno-Economic Analysis of CO_2 Electrolysis Systems. *Ind. Eng. Chem. Res.* **2018**, *57* (6), 2165–2177. https://doi.org/10.1021/acs.iecr.7b03514.
(22) Grice, K. A. Carbon Dioxide Reduction with Homogenous Early Transition Metal Complexes: Opportunities and Challenges for Developing CO 2 Catalysis. *Coordination Chemistry Reviews* **2017**, *336*, 78–95. https://doi.org/10.1016/j.ccr.2017.01.007.
(23) Yu, H.; Wu, H.; Chow, Y. L.; Wang, J.; Zhang, J. Revolutionizing Electrochemical CO_2 Reduction to Deeply Reduced Products on Non-Cu-Based Electrocatalysts. *Energy Environ. Sci.* **2024**, 10.1039.D4EE01301H. https://doi.org/10.1039/D4EE01301H.
(24) Elgrishi, N.; Rountree, K. J.; McCarthy, B. D.; Rountree, E. S.; Eisenhart, T. T.; Dempsey, J. L. A Practical Beginner's Guide to Cyclic Voltammetry. *J. Chem. Educ.* **2018**, *95* (2), 197–206. https://doi.org/10.1021/acs.jchemed.7b00361.
(25) Potter, M.; Smith, D. E.; Armstrong, C. G.; Toghill, K. E. Electrochemically Decoupled Reduction of CO_2 to Formate over a Dispersed Heterogeneous Bismuth Catalyst Enabled *via* Redox Mediators. *EES. Catal.* **2024**, *2* (1), 379–388. https://doi.org/10.1039/D3EY00271C.
(26) Lu, Y.; Han, B.; Tian, C.; Wu, J.; Geng, D.; Wang, D. Efficient Electrocatalytic Reduction of CO2 to CO on an Electrodeposited Zn Porous Network. *Electrochemistry Communications* **2018**, *97*, 87–90. https://doi.org/10.1016/j.elecom.2018.11.002.
(27) Jhong, H.-R. "Molly"; Ma, S.; Kenis, P. J. Electrochemical Conversion of CO2 to Useful Chemicals: Current Status, Remaining Challenges, and Future

Opportunities. *Current Opinion in Chemical Engineering* **2013**, *2* (2), 191–199. https://doi.org/10.1016/j.coche.2013.03.005.
(28) Jiang, Z.; Xiao, T.; Kuznetsov, V. L.; Edwards, P. P. Turning Carbon Dioxide into Fuel. *Phil. Trans. R. Soc. A.* **2010**, *368* (1923), 3343–3364. https://doi.org/10.1098/rsta.2010.0119.
(29) Whipple, D. T.; Kenis, P. J. A. Prospects of CO_2 Utilization via Direct Heterogeneous Electrochemical Reduction. *J. Phys. Chem. Lett.* **2010**, *1* (24), 3451–3458. https://doi.org/10.1021/jz1012627.
(30) Lin, R.; Guo, J.; Li, X.; Patel, P.; Seifitokaldani, A. Electrochemical Reactors for CO2 Conversion. *Catalysts* **2020**, *10* (5), 473. https://doi.org/10.3390/catal10050473.
(31) Saxena, A.; Liyanage, W.; Masud, J.; Kapila, S.; Nath, M. Selective Electroreduction of CO_2 to Carbon-Rich Products with a Simple Binary Copper Selenide Electrocatalyst. *J. Mater. Chem. A* **2021**, *9* (11), 7150–7161. https://doi.org/10.1039/D0TA11518E.
(32) Reichert, J.; Brunner, B.; Jess, A.; Wasserscheid, P.; Albert, J. Biomass Oxidation to Formic Acid in Aqueous Media Using Polyoxometalate Catalysts – Boosting FA Selectivity by in-Situ Extraction. *Energy Environ. Sci.* **2015**, *8* (10), 2985–2990. https://doi.org/10.1039/C5EE01706H.
(33) Shao, H.; Muduli, S. K.; Tran, P. D.; Soo, H. S. Enhancing Electrocatalytic Hydrogen Evolution by Nickel Salicylaldimine Complexes with Alkali Metal Cations in Aqueous Media. *Chem. Commun.* **2016**, *52* (14), 2948–2951. https://doi.org/10.1039/C5CC09456A.
(34) Kong, Q.; An, X.; Liu, Q.; Xie, L.; Zhang, J.; Li, Q.; Yao, W.; Yu, A.; Jiao, Y.; Sun, C. Copper-Based Catalysts for the Electrochemical Reduction of Carbon Dioxide: Progress and Future Prospects. *Mater. Horiz.* **2023**, *10* (3), 698–721. https://doi.org/10.1039/D2MH01218A.
(35) Costentin, C.; Robert, M.; Savéant, J.-M. Catalysis of the Electrochemical Reduction of Carbon Dioxide. *Chem. Soc. Rev.* **2013**, *42* (6), 2423–2436. https://doi.org/10.1039/C2CS35360A.
(36) Diercks, C. S.; Lin, S.; Kornienko, N.; Kapustin, E. A.; Nichols, E. M.; Zhu, C.; Zhao, Y.; Chang, C. J.; Yaghi, O. M. Reticular Electronic Tuning of Porphyrin Active Sites in Covalent Organic Frameworks for Electrocatalytic Carbon Dioxide Reduction. *J. Am. Chem. Soc.* **2018**, *140* (3), 1116–1122. https://doi.org/10.1021/jacs.7b11940.
(37) Zhang, L.; Merino-Garcia, I.; Albo, J.; Sánchez-Sánchez, C. M. Electrochemical CO2 Reduction Reaction on Cost-Effective Oxide-Derived Copper and Transition Metal–Nitrogen–Carbon Catalysts. *Current Opinion in Electrochemistry* **2020**, *23*, 65–73. https://doi.org/10.1016/j.coelec.2020.04.005.
(38) Oh, Y.; Hu, X. Organic Molecules as Mediators and Catalysts for Photocatalytic and Electrocatalytic CO_2 Reduction. *Chem. Soc. Rev.* **2013**, *42* (6), 2253–2261. https://doi.org/10.1039/C2CS35276A.
(39) Wang, X.; Yu, M.; Feng, X. Electronic Structure Regulation of Noble Metal-Free Materials toward Alkaline Oxygen Electrocatalysis. *eScience* **2023**, *3* (4), 100141. https://doi.org/10.1016/j.esci.2023.100141.
(40) Sowmiah, S.; Esperança, J. M. S. S.; Rebelo, L. P. N.; Afonso, C. A. M. Pyridinium Salts: From Synthesis to Reactivity and Applications. *Org. Chem. Front.* **2018**, *5* (3), 453–493. https://doi.org/10.1039/C7QO00836H.

(41) Dalton, T.; Faber, T.; Glorius, F. C–H Activation: Toward Sustainability and Applications. *ACS Cent. Sci.* **2021**, *7* (2), 245–261. https://doi.org/10.1021/acscentsci.0c01413.
(42) Hartwig, J. F. Evolution of C–H Bond Functionalization from Methane to Methodology. *J. Am. Chem. Soc.* **2016**, *138* (1), 2–24. https://doi.org/10.1021/jacs.5b08707.
(43) Lucio, A. J.; Shaw, S. K. Pyridine and Pyridinium Electrochemistry on Polycrystalline Gold Electrodes and Implications for CO_2 Reduction. *J. Phys. Chem. C* **2015**, *119* (22), 12523–12530. https://doi.org/10.1021/acs.jpcc.5b03355.
(44) Liao, K.; Askerka, M.; Zeitler, E. L.; Bocarsly, A. B.; Batista, V. S. Electrochemical Reduction of Aqueous Imidazolium on Pt(111) by Proton Coupled Electron Transfer. *Top Catal* **2015**, *58* (1), 23–29. https://doi.org/10.1007/s11244-014-0340-2.
(45) Benson, E. E.; Kubiak, C. P.; Sathrum, A. J.; Smieja, J. M. Electrocatalytic and Homogeneous Approaches to Conversion of CO_2 to Liquid Fuels. *Chem. Soc. Rev.* **2009**, *38* (1), 89–99. https://doi.org/10.1039/B804323J.
(46) An, X.; Wang, P.; Ma, X.; Du, X.; Hao, X.; Yang, Z.; Guan, G. Application of Ionic Liquids in CO2 Capture and Electrochemical Reduction: A Review. *Carbon Resources Conversion* **2023**, *6* (2), 85–97. https://doi.org/10.1016/j.crcon.2023.02.003.
(47) DiMeglio, J. L.; Rosenthal, J. Selective Conversion of CO_2 to CO with High Efficiency Using an Inexpensive Bismuth-Based Electrocatalyst. *J. Am. Chem. Soc.* **2013**, *135* (24), 8798–8801. https://doi.org/10.1021/ja4033549.
(48) Wu, Y.; Jiang, J.; Weng, Z.; Wang, M.; Broere, D. L. J.; Zhong, Y.; Brudvig, G. W.; Feng, Z.; Wang, H. Electroreduction of CO_2 Catalyzed by a Heterogenized Zn–Porphyrin Complex with a Redox-Innocent Metal Center. *ACS Cent. Sci.* **2017**, *3* (8), 847–852. https://doi.org/10.1021/acscentsci.7b00160.
(49) Pirzada, B. M.; Dar, A. H.; Shaikh, M. N.; Qurashi, A. Reticular-Chemistry-Inspired Supramolecule Design as a Tool to Achieve Efficient Photocatalysts for CO_2 Reduction. *ACS Omega* **2021**, *6* (44), 29291–29324. https://doi.org/10.1021/acsomega.1c04018.
(50) Lim, C.-H.; Holder, A. M.; Musgrave, C. B. Mechanism of Homogeneous Reduction of CO_2 by Pyridine: Proton Relay in Aqueous Solvent and Aromatic Stabilization. *J. Am. Chem. Soc.* **2013**, *135* (1), 142–154. https://doi.org/10.1021/ja3064809.
(51) Aikens, D. A. Electrochemical Methods, Fundamentals and Applications. *J. Chem. Educ.* **1983**, *60* (1), A25. https://doi.org/10.1021/ed060pA25.1.
(52) Wang, L.; Nitopi, S. A.; Bertheussen, E.; Orazov, M.; Morales-Guio, C. G.; Liu, X.; Higgins, D. C.; Chan, K.; Nørskov, J. K.; Hahn, C.; Jaramillo, T. F. Electrochemical Carbon Monoxide Reduction on Polycrystalline Copper: Effects of Potential, Pressure, and pH on Selectivity toward Multicarbon and Oxygenated Products. *ACS Catal.* **2018**, *8* (8), 7445–7454. https://doi.org/10.1021/acscatal.8b01200.
(53) Boutin, E.; Salamé, A.; Robert, M. Confined Molecular Catalysts Provide an Alternative Interpretation to the Electrochemically Reversible Demetallation of Copper Complexes. *Nat Commun* **2022**, *13* (1), 4190. https://doi.org/10.1038/s41467-022-31661-1.

(54) Li, Y.; Wang, K.; He, X. Recent Progress of Electron-Withdrawing-Group-Tethered Arenes Involved Asymmetric Nucleophilic Aromatic Functionalizations. *Adv Synth Catal* **2022**, *364* (21), 3630–3650. https://doi.org/10.1002/adsc.202200835.
(55) Xie, W.-J.; Mulina, O. M.; Terent'ev, A. O.; He, L.-N. Metal–Organic Frameworks for Electrocatalytic CO2 Reduction into Formic Acid. *Catalysts* **2023**, *13* (7), 1109. https://doi.org/10.3390/catal13071109.
(56) Pal, P. Arsenic Removal by Membrane Distillation. In *Groundwater Arsenic Remediation*; Elsevier, 2015; pp 179–270. https://doi.org/10.1016/B978-0-12-801281-9.00005-9.
(57) Compton, R. G.; Banks, C. E. *Understanding Voltammetry*, 2nd ed.; IMPERIAL COLLEGE PRESS, 2010. https://doi.org/10.1142/p726.
(58) Bollo, S.; Finger, S.; Sturm, J. C.; Núñez-Vergara, L. J.; Squella, J. A. Cyclic Voltammetry and Scanning Electrochemical Microscopy Studies of the Heterogeneous Electron Transfer Reaction of Some Nitrosoaromatic Compounds. *Electrochimica Acta* **2007**, *52* (15), 4892–4898. https://doi.org/10.1016/j.electacta.2007.01.003.
(59) Gritzner, G.; Kůta, J. Recommendations on Reporting Electrode Potentials in Nonaqueous Solvents. *Electrochimica Acta* **1984**, *29* (6), 869–873. https://doi.org/10.1016/0013-4686(84)80027-4.
(60) Wang, W.; Zhang, J.; Wang, H.; Chen, L.; Bian, Z. Photocatalytic and Electrocatalytic Reduction of CO2 to Methanol by the Homogeneous Pyridine-Based Systems. *Applied Catalysis A: General* **2016**, *520*, 1–6. https://doi.org/10.1016/j.apcata.2016.04.003.
(61) Peroff, A. G.; Weitz, E.; Van Duyne, R. P. Mechanistic Studies of Pyridinium Electrochemistry: Alternative Chemical Pathways in the Presence of CO_2. *Phys. Chem. Chem. Phys.* **2016**, *18* (3), 1578–1586. https://doi.org/10.1039/C5CP04757A.
(62) Keith, J. A.; Carter, E. A. Electrochemical Reactivities of Pyridinium in Solution: Consequences for CO2 Reduction Mechanisms. *Chem. Sci.* **2013**, *4* (4), 1490. https://doi.org/10.1039/c3sc22296a.
(63) Edwards, J. P.; Xu, Y.; Gabardo, C. M.; Dinh, C.-T.; Li, J.; Qi, Z.; Ozden, A.; Sargent, E. H.; Sinton, D. Efficient Electrocatalytic Conversion of Carbon Dioxide in a Low-Resistance Pressurized Alkaline Electrolyzer. *Applied Energy* **2020**, *261*, 114305. https://doi.org/10.1016/j.apenergy.2019.114305.
(64) Stasyuk, O. A.; Szatylowicz, H.; Krygowski, T. M.; Fonseca Guerra, C. How Amino and Nitro Substituents Direct Electrophilic Aromatic Substitution in Benzene: An Explanation with Kohn–Sham Molecular Orbital Theory and Voronoi Deformation Density Analysis. *Phys. Chem. Chem. Phys.* **2016**, *18* (17), 11624–11633. https://doi.org/10.1039/C5CP07483E.
(65) Hu, Y.; Cheng, K.; He, L.; Zhang, X.; Jiang, B.; Jiang, L.; Li, C.; Wang, G.; Yang, Y.; Liu, M. NMR-Based Methods for Protein Analysis. *Anal. Chem.* **2021**, *93* (4), 1866–1879. https://doi.org/10.1021/acs.analchem.0c03830.
(66) Carbajo, R. J.; Neira, J. L. The Basis of Nuclear Magnetic Resonance Spectroscopy. In *NMR for Chemists and Biologists*; SpringerBriefs in Biochemistry and Molecular Biology; Springer Netherlands: Dordrecht, 2013; pp 1–29. https://doi.org/10.1007/978-94-007-6976-2_1.

(67) Jacobsen, N. E. *NMR Spectroscopy Explained: Simplified Theory, Applications and Examples for Organic Chemistry and Structural Biology*, 1st ed.; Wiley, 2007. https://doi.org/10.1002/9780470173350.

Acknowledgment:

I would like to express my deepest gratitude to my supervisor, Professor Graham, for his invaluable guidance, support, and encouragement throughout this research. His expertise and mentorship have been instrumental in shaping this work.

I would also like to thank my postdoc, Dr. William, for his insightful advice, constant assistance, and availability to help whenever I needed it.

A special thanks to Margaret, Noor, Mohammed and the NAMI group for their ongoing support, encouragement, and collaboration throughout the journey.

I also extend my sincerest thanks to my beloved husband, Mohammed, for his love, patience, and constant support. To my dear son, Abdualmalik, and my lovely daughter, Deema, your love and inspiration have been my greatest motivation.

To my mom and dad, and my entire family, and to my dear friends thank you for your endless love, belief in me, and encouragement. Your support has been the foundation of my success, and I am forever grateful.